

# Probing non-standard neutrino interactions with supernova neutrinos

A. Esteban-Pretel, R. Tomàs and J. W. F. Valle<sup>1</sup>

<sup>1</sup>*AHEP Group, Institut de Física Corpuscular - C.S.I.C./Universitat de València  
Edifici Instituts d'Investigació, Apt. 22085, E-46071 València, Spain*

(Dated: November 4, 2018)

We analyze the possibility of probing non-standard neutrino interactions (NSI, for short) through the detection of neutrinos produced in a future galactic supernova (SN). We consider the effect of NSI on the neutrino propagation through the SN envelope within a three-neutrino framework, paying special attention to the inclusion of NSI-induced resonant conversions, which may take place in the most deleptonised inner layers. We study the possibility of detecting NSI effects in a Megaton water Cherenkov detector, either through modulation effects in the  $\bar{\nu}_e$  spectrum due to (i) the passage of shock waves through the SN envelope, (ii) the time dependence of the electron fraction and (iii) the Earth matter effects; or, finally, through the possible detectability of the neutronization  $\nu_e$  burst. We find that the  $\bar{\nu}_e$  spectrum can exhibit dramatic features due to the internal NSI-induced resonant conversion. This occurs for non-universal NSI strengths of a few %, and for very small flavor-changing NSI above a few  $\times 10^{-5}$ .

PACS numbers: 13.15.+g, 14.60.Lm, 14.60.Pq, 14.60.St, 97.60.Bw

## I. INTRODUCTION

The very first data of the KamLAND collaboration [1] have been enough to isolate neutrino oscillations as the correct mechanism explaining the solar neutrino problem [2, 3], indicating also that large mixing angle (LMA) was the right solution. The 766.3 ton-yr KamLAND data sample further strengthens the validity of the LMA oscillation interpretation of the data [4].

Current data imply that neutrino have mass. For an updated review of the current status of neutrino oscillations see [5]. Theories of neutrino mass [6, 7] typically require that neutrinos have non-standard properties such as neutrino electromagnetic transition moments [8, 9, 10] or non-standard four-Fermi interactions (NSI, for short) [11, 12, 13]. The expected magnitude of the NSI effects is rather model-dependent.

Seesaw-type models lead to a non-trivial structure of the lepton mixing matrix characterizing the charged and neutral current weak interactions [6]. The NSI which are induced by the charged and neutral current gauge interactions may be sizeable [14, 15, 16, 17, 18]. Alternatively, non-standard neutrino interactions may arise in models where neutrinos masses are radiatively “calculable” [19, 20]. Finally, in some supersymmetric unified models, the strength of non-standard neutrino interac-

tions may arise from renormalization and/or threshold effects [21].

We stress that non-standard interactions strengths are highly model-dependent. In some models NSI strengths are too small to be relevant for neutrino propagation, because they are either suppressed by some large mass scale or restricted by limits on neutrino masses, or both. However, this need not be the case, and there are many theoretically attractive scenarios where moderately large NSI strengths are possible and consistent with the smallness of neutrino masses. In fact one can show that NSI may exist even in the limit of massless neutrinos [14, 15, 16, 17, 18]. Such may also occur in the context of fully unified models like  $SO(10)$  [22].

We argue that, in addition to the precision determination of the oscillation parameters, it is necessary to test for sub-leading non-oscillation effects that could arise from non-standard neutrino interactions. These are natural outcome of many neutrino mass models and can be of two types: flavor-changing (FC) and non-universal (NU). These are constrained by existing experiments (see below) and, with neutrino experiments now entering a precision phase [23], an improved determination of neutrino parameters and their theoretical impact constitute an important goal in astroparticle and high energy physics [5].

Here we concentrate on the impact of non-standard

neutrino interactions on supernova physics. We show how complementary information on the NSI parameters could be inferred from the detection of core-collapse supernova neutrinos. The motivation for the study is twofold. First, if a future SN event takes place in our Galaxy the number of neutrino events expected in the current or planned neutrino detectors would be enormous,  $\mathcal{O}(10^4 - 10^5)$  [24]. Moreover, the extreme conditions under which neutrinos have to travel since they are created in the SN core, in strongly deleptonised regions at nuclear densities, until they reach the Earth, lead to strong matter effects. In particular the effect of small values of the NSI parameters can be dramatically enhanced, possibly leading to observable consequences.

This paper is planned as follows. In Sec. II we summarize the current observational bounds on the parameters describing the NSI, including previous works on NSI in SNe. In Sec. III we describe the neutrino propagation formalism as well as the SN profiles which will be used. In Sec. IV we analyze the effect of NSI on the  $\nu$  propagation in the inner regions near the neutrinosphere and in the outer regions of the SN envelope. In Sec. V we discuss the possibility of using various observables to probe the presence of NSI in the neutrino signal of a future galactic SN. Finally in Sec. VI we present our conclusions.

## II. PRELIMINARIES

A large class of non-standard interactions may be parametrized with the effective low-energy four-fermion operator:

$$\mathcal{L}_{NSI} = -\varepsilon_{\alpha\beta}^{fP} 2\sqrt{2}G_F (\bar{\nu}_\alpha \gamma_\mu L \nu_\beta) (\bar{f} \gamma^\mu P f), \quad (1)$$

where  $P = L, R$  and  $f$  is a first generation fermion:  $e, u, d$ . The coefficients  $\varepsilon_{\alpha\beta}^{fP}$  denote the strength of the NSI between the neutrinos of flavors  $\alpha$  and  $\beta$  and the  $P$ -handed component of the fermion  $f$ .

Current constraints on  $\varepsilon_{\alpha\beta}^{fP}$  come from a variety of different sources, which we now briefly list.

### A. Laboratory

Neutrino scattering experiments [25, 26, 27, 28, 29] provide the following bounds,  $|\varepsilon_{\mu\mu}^{fP}| \lesssim 10^{-3} -$

$10^{-2}$ ,  $|\varepsilon_{ee}^{fP}| \lesssim 10^{-1} - 1$ ,  $|\varepsilon_{\mu\tau}^{fP}| \lesssim 0.05$ ,  $|\varepsilon_{e\tau}^{fP}| \lesssim 0.5$  at 90 % C.L [30, 31, 32]. On the other hand the analysis of the  $e^+e^- \rightarrow \nu\bar{\nu}\gamma$  cross section measured at LEP II leads to a bound on  $|\varepsilon_{\tau\tau}^{eP}| \lesssim 0.5$  [33]. Future prospects to improve the current limits imply the measurement of  $\sin^2 \vartheta_W$  leptonically in the scattering off electrons in the target, as well as in neutrino deep inelastic scattering in a future neutrino factory. The main improvement would be in the case of  $|\varepsilon_{ee}^{fP}|$  and  $|\varepsilon_{e\tau}^{fP}|$ , where values as small as  $10^{-3}$  and 0.02, respectively, could be reached [31].

The search for flavor violating processes involving charged leptons is expected to restrict corresponding neutrino interactions, to the extent that the  $SU(2)$  gauge symmetry is assumed. However, this can at most give indicative order-of-magnitude restrictions, since we know  $SU(2)$  is not a good symmetry of nature. Using radiative corrections it has been argued that, for example,  $\mu - e$  conversion on nuclei like in the case of  $\mu^-Ti$  also constrains  $|\varepsilon_{\mu e}^{qP}| \lesssim 7.7 \times 10^{-4}$  [31].

Non-standard interactions can also affect neutrino propagation through matter, probed in current neutrino oscillation experiments. The bounds so obtained apply to the vector coupling constant of the NSI,  $\varepsilon_{\alpha\beta}^{fV} = \varepsilon_{\alpha\beta}^{fL} + \varepsilon_{\alpha\beta}^{fR}$ , since only this appears in neutrino propagation in matter [91].

### B. Solar and reactor

The role of neutrino NSIs as subleading effects on the solar neutrino oscillations and KamLAND has been recently considered in Ref. [34, 35, 36] with the following bounds at 90 % CL for  $\varepsilon \equiv -\sin \vartheta_{23} \varepsilon_{e\tau}^{dV}$  with the allowed range  $-0.93 \lesssim \varepsilon \lesssim 0.30$ , while for the diagonal term  $\varepsilon' \equiv \sin^2 \vartheta_{23} \varepsilon_{\tau\tau}^{dV} - \varepsilon_{ee}^{dV}$ , the only forbidden region is  $[0.20, 0.78]$  [36]. Only in the ideal case of infinitely precise solar neutrino oscillation parameters determination, the allowed range would “close from the left” for negative NSI parameter values, at  $-0.6$  for  $\varepsilon$  and  $-0.7$  for  $\varepsilon'$ .

### C. Atmospheric and accelerator neutrinos

Non-standard interactions involving muon neutrinos can be constrained by atmospheric neutrino experiments as well as accelerator neutrino oscillation searches at

K2K and MINOS. In Ref. [37] Super-Kamiokande and MACRO observations of atmospheric neutrinos were considered in the framework of two neutrinos. The limits obtained were  $-0.05 \lesssim \varepsilon_{\mu\tau}^{dV} < 0.04$  and  $|\varepsilon_{\tau\tau}^{dV} - \varepsilon_{\mu\mu}^{dV}| \lesssim 0.17$  at 99 % CL. The same data set together with K2K were recently considered in Refs. [38, 39] to study the nonstandard neutrino interactions in a three generation scheme under the assumption  $\varepsilon_{e\mu} = \varepsilon_{\mu\mu} = \varepsilon_{\mu\tau} = 0$ . The allowed region of  $\varepsilon_{\tau\tau}$  obtained for values of  $\varepsilon_{e\tau}$  smaller than  $\mathcal{O}(10^{-1})$  becomes  $\Sigma_{f=u,d,e} \varepsilon_{\alpha\beta}^{fV} N_f / N_e \lesssim 0.2$  [39], where  $N_f$  stands for the fermion number density.

#### D. Cosmology

If non-standard interactions with electrons were large they might also lead to important cosmological and astrophysical implications. For instance, neutrinos could be kept in thermal contact with electrons and positrons longer than in the standard case, hence they would share a larger fraction of the entropy release from  $e^\pm$  annihilations. This would affect the predicted features of the cosmic background of neutrinos. As recently pointed out in Ref [40] required couplings are, though, larger than the current laboratory bounds.

#### E. NSI in Supernovae

According to the currently accepted supernova (SN) paradigm, neutrinos are expected to play a crucial role in SN dynamics. As a result, SN physics provides a laboratory to probe neutrino properties. Moreover, many future large neutrino detectors are currently being discussed [41]. The enormous number of events,  $\mathcal{O}(10^4 - 10^5)$  that would be “seen” in these detectors indicates that a future SN in our Galaxy would provide a very sensitive probe of non-standard neutrino interaction effects.

The presence of NSI can lead to important consequences for the SN neutrino physics both in the highly dense core as well as in the envelope where neutrinos basically freely stream.

The role of non-forward neutrino scattering processes on heavy nuclei and free nucleons giving rise to flavor change within the SN core has been recently analyzed in

Ref. [42, 43]. The main effect found was a reduction in the core electron fraction  $Y_e$  during core collapse. A lower  $Y_e$  would lead to a lower homologous core mass, a lower shock energy, and a greater nuclear photon-disintegration burden for the shock wave. By allowing a maximum  $\Delta Y_e = -0.02$  it has been claimed that  $\varepsilon_{e\alpha} \lesssim 10^{-3}$ , where  $\alpha = \mu, \tau$  [43].

On the other hand it has been noted since long ago that the existence of NSI plays an important role in the propagation of SN neutrinos through the envelope leading to the possibility of a new resonant conversion. In contrast to the well known MSW effect [44, 45] it would take place even for massless neutrinos [13]. Two basic ingredients are necessary: universal and flavor changing NSI. In the original scheme neutrinos were mixed in the leptonic charged current and universality was violated thanks to the effect of mixing with heavy gauge singlet leptons [6, 14]. Such resonance would induce strong neutrino flavor conversion both for neutrinos and antineutrinos simultaneously, possibly affecting the neutrino signal of the SN1987A as well as the possibility of having  $r$ -process nucleosynthesis. This was first quantitatively considered within a two-flavor  $\nu_e - \nu_\tau$  scheme, and bounds on the relevant NSI parameters were obtained using both arguments [46].

One of the main features of the such “internal” or “massless” resonant conversion mechanism is that it requires the violation of universality, its position being determined only by the matter chemical composition, namely the value of the electron fraction  $Y_e$ , and not by the density. In view of the experimental upper bounds on the NSI parameters such new resonance can only take place in the inner layers of the supernova, near the neutrinosphere, where  $Y_e$  takes its minimum values. In this region the values of  $Y_e$  are small enough to allow for resonance conversions to take place in agreement with existing bounds on the strengths of non-universal NSI parameters.

The SN physics implications of another type of NSI present in supersymmetric R-parity violating models have also been studied in Ref. [47], again for a system of two neutrinos. For definiteness NSI on  $d$ -quarks were considered, in two cases: (i) massless neutrinos without mixing in the presence of flavor-changing (FC) and non-universal (NU) NSIs, and (ii) neutrinos with eV masses

and FC NSI. Different arguments have been used in order to constrain the parameters describing the NSI, namely, the SN1987A signal, the possibility to get successful  $r$ -process nucleosynthesis, and the possible enhancement of the energy deposition behind the shock wave to reactivate it.

On the other hand several subsequent articles [48, 49, 50] considered the effects of NSI on the neutrino propagation in a three-neutrino mixing scenario for the case  $Y_e > 0.4$ , typical for the outer SN envelope. Together with the assumption that  $\varepsilon_{\alpha\beta}^{dV} \lesssim 10^{-2}$  this prevents the appearance of internal resonances in contrast to previous references.

Motivated by supersymmetric theories without R parity, in Ref. [48] the authors considered the effects of small-strength NSI with  $d$ -quarks. Following the formalism developed in Refs. [51, 52] they studied the corrections that such NSI would have on the expressions for the survival probabilities in the standard resonances MSW-H and MSW-L. A similar analysis was performed in Ref. [49] assuming Z-induced NSI interactions originated by additional heavy neutrinos. A phenomenological generalization of these results was carried out in Ref. [50]. The authors found an analytical compact expression for the survival probabilities in which the main effects of the NSI can be embedded through shifts of the mixing angles  $\vartheta_{12}$  and  $\vartheta_{13}$ . In contrast to similar expressions found previously these directly apply to all mixing angles, and in the case with Earth matter effects. The main phenomenological consequence was the identification of a degeneracy between  $\vartheta_{13}$  and  $\varepsilon_{e\alpha}$ , similar to the analogous “confusion” between  $\vartheta_{13}$  and the corresponding NSI parameter noted to exist in the context of long-baseline neutrino oscillations [53, 54].

We have now re-considered the general three-neutrino mixing scenario with NSI. In contrast to previous work [48, 49, 50], we have not restricted ourselves to large values of  $Y_e$ , discussing also small values present in the inner layers. This way our generalized description includes both the possibility of neutrinos having the “massless” NSI-induced resonant conversions in the inner layers of the SN envelope [13, 46, 47], as well as the “outer” oscillation-induced conversions [48, 49, 50] [92].

### III. NEUTRINO EVOLUTION

In this section we describe the main ingredients of our analysis. Our emphasis will be on the use of astrophysically realistic SN matter and  $Y_e$  profiles, characterizing its density and the matter composition. Their details, in particular their time dependence, are crucial in determining the way the non-standard neutrino interactions affect the propagation of neutrinos in the SN medium.

#### A. Evolution Equation

As discussed in Sec. II in an unpolarized medium the neutrino propagation in matter will be affected by the vector coupling constant of the NSI,  $\varepsilon_{\alpha\beta}^{fV} = \varepsilon_{\alpha\beta}^{fL} + \varepsilon_{\alpha\beta}^{fR}$  [93]. The way the neutral current NSI modifies the neutrino evolution will be parametrized phenomenologically through the effective low-energy four-fermion operator described in Eq. (1). We also assume  $\varepsilon_{\alpha\beta}^f \in \mathfrak{R}$ , neglecting possible  $CP$  violation in the new interactions.

Under these assumptions the Hamiltonian describing the SN neutrino evolution in the presence of NSI can be cast in the following form [94]

$$i \frac{d}{dr} \nu_\alpha = (H_{\text{kin}} + H_{\text{int}})_{\alpha\beta} \nu_\beta, \quad (2)$$

where  $H_{\text{kin}}$  stands for the kinetic term

$$H_{\text{kin}} = U \frac{M^2}{2E} U^\dagger, \quad (3)$$

with  $M^2 = \text{diag}(m_1^2, m_2^2, m_3^2)$ , and  $U$  the three-neutrino lepton mixing matrix [6] in the PDG convention [55] and with no  $CP$  phases.

The second term of the Hamiltonian accounts for the interaction of neutrinos with matter and can be split into two pieces,

$$H_{\text{int}} = H_{\text{int}}^{\text{std}} + H_{\text{int}}^{\text{nsi}}. \quad (4)$$

The first term,  $H_{\text{int}}^{\text{std}}$  describes the standard interaction with matter and can be written as  $H_{\text{int}}^{\text{std}} = \text{diag}(V_{CC}, 0, 0)$  up to one loop corrections due to different masses of the muon and tau leptons [56]. The standard matter potential for neutrinos is given by

$$V_{CC} = \sqrt{2} G_F N_e = V_0 \rho Y_e, \quad (5)$$

where  $V_0 \approx 7.6 \times 10^{-14}$  eV, the density is given in  $\text{g}/\text{cm}^3$ , and  $Y_e$  stands for the relative number of electrons with respect to baryons. For antineutrinos the potential is identical but with the sign changed.

The term in the Hamiltonian describing the non-standard neutrino interactions with a fermion  $f$  can be expressed as,

$$(H_{\text{int}}^{\text{nsi}})_{\alpha\beta} = \sum_{f=e,u,d} (V_{\text{nsi}}^f)_{\alpha\beta}, \quad (6)$$

with  $(V_{\text{nsi}}^f)_{\alpha\beta} \equiv \sqrt{2}G_F N_f \varepsilon_{\alpha\beta}^f$ . For definiteness and motivated by actual models, for example, those with broken R parity supersymmetry we take for  $f$  the down-type quark. However, an analogous treatment would apply to the case of NSI on up-type quarks, the existence of NSI with electrons brings no drastic qualitative differences with respect to the pure oscillation case (see below). Therefore the NSI potential can be expressed as follows,

$$(V_{\text{nsi}}^d)_{\alpha\beta} = \varepsilon_{\alpha\beta}^d V_0 \rho (2 - Y_e). \quad (7)$$

From now on we will not explicitly write the superindex  $d$ . In order to further simplify the problem we will redefine the diagonal NSI parameters so that  $\varepsilon_{\mu\mu} = 0$ , as one can easily see that subtracting a matrix proportional to the identity leaves the physics involved in the neutrino oscillation unaffected.

## B. Supernova matter profiles

Neutrino propagation depends on the supernova matter and chemical profile through the effective potential. This profile exhibits an important time dependence during the explosion. Fig. 1 shows the density  $\rho(t, r)$  and the electron fraction  $Y_e(t, r)$  profiles for the SN progenitor as well as at different times post-bounce.

Progenitor density profiles can be roughly parametrized by a power-law function

$$\rho(r) = \rho_0 \left( \frac{R_0}{r} \right)^n, \quad (8)$$

where  $\rho_0 \sim 10^4$   $\text{g}/\text{cm}^3$ ,  $R_0 \sim 10^9$  cm, and  $n \sim 3$ . The electron fraction profile varies depending on the matter composition of the different layers. For instance, typical values of  $Y_e$  between 0.42 and 0.45 in the inner regions

are found in stellar evolution simulations [57]. In the intermediate regions, where the MSW  $H$  and  $L$ -resonances take place  $Y_e \approx 0.5$ . This value can further increase in the most outer layers of the SN envelope due to the presence of hydrogen.

After the SN core bounce the matter profile is affected in several ways. First note that a front shock wave starts to propagate outwards and eventually ejects the SN envelope. The evolution of the shock wave will strongly modify the density profile and therefore the neutrino propagation [58, 59]. Following Ref. [60] we shall assume that the structure of the shock wave is more complicated and an additional “reverse wave” appears due to the collision of the neutrino-driven wind and the slowly moving material behind the forward shock, as seen in the upper panel of Fig. 1 [95].

On the other hand, the electron fraction is also affected by the time evolution as the SN explosion proceeds. Once the collapse starts the core density grows so that the neutrinos become eventually effectively trapped within the so called “neutrinosphere”. At this point the trapped electron fraction has decreased until values of the order of 0.33 [61]. When the inner core reaches the nuclear density it can not contract any further and bounces. As a consequence a shock wave forms in the inner core and starts propagating outwards. When the newly formed supernova shock reaches densities low enough for the initially trapped neutrinos to begin streaming faster than the shock propagates [62], a breakout pulse of  $\nu_e$  is launched. In the shock-heated matter, which is still rich of electrons and completely disintegrated into free neutrons and protons, a large number of  $\nu_e$  are rapidly produced by electron captures on protons. They follow the shock on its way out until they are released in a very luminous flash, the breakout burst, at about the moment when the shock penetrates the neutrinosphere and the neutrinos can escape essentially unhindered. As a consequence, the lepton number in the layer around the neutrinosphere decreases strongly and the matter neutronizes [63]. The value of  $Y_e$  steadily decreases in these layers until values of the order of  $\mathcal{O}(10^{-2})$ . Outside the neutrinosphere there is a steep rise until  $Y_e \approx 0.5$ . This is a robust feature of the neutrino-driven baryonic wind. Neutrino heating drives the wind mass loss and causes  $Y_e$  to rise within a few 10 km from low to high values, between 0.45

and 0.55 [64], see bottom panel of Fig. 1. Inspired in the numerical results of Ref. [60] we have parametrized the behavior of the electron fraction near the neutrinosphere phenomenologically as,

$$Y_e = a + b \arctan[(r - r_0)/r_s], \quad (9)$$

where  $a \approx 0.23 - 0.26$  and  $b \approx 0.16 - 0.20$ . The parameters  $r_0$  and  $r_s$  describe where the rise takes place and how steep it is, respectively. As can be seen in Fig. 1 both decrease with time.

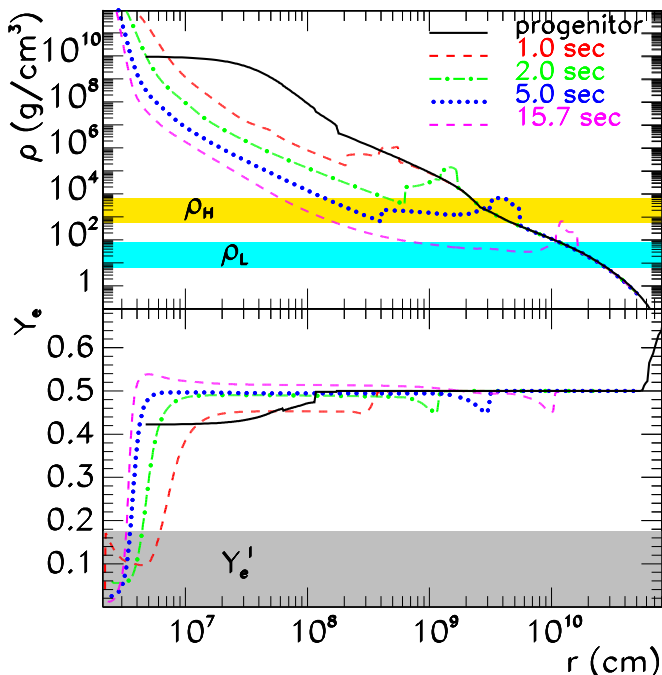


FIG. 1: Density (upper panel) and electron fraction (bottom panel) profiles for the SN progenitor and at different instants after the core bounce, from Ref. [60]. The regions where the  $H$  (yellow) and the  $L$  (cyan) resonance take place are also indicated, as well as the NSI-induced  $I$  (gray) resonance for the parameters  $\varepsilon_{ee} = 0$ ,  $\varepsilon_{\tau\tau} \lesssim 0.07$  and  $|\varepsilon_{\mu\tau}| \lesssim 0.05$

#### IV. THE TWO REGIMES

In order to study the neutrino propagation through the SN envelope we will split the problem into two different regions: the inner envelope, defined by the condition  $V_{CC} \gg \Delta m_{\text{atm}}^2/(2E)$  with  $\Delta m_{\text{atm}}^2 \equiv m_3^2 - m_2^2$ , and the outer one, where  $\Delta m_{\text{atm}}^2/(2E) \gtrsim V_{CC}$ . From the upper panel of Fig. 1 one can see how the boundary roughly

varies between  $r \approx 10^8$  cm and  $10^9$  cm, depending on the time considered. This way one can fully characterize all resonances that can take place in the propagation of supernova neutrinos, both the outer resonant conversions related to neutrino masses and indicated as the upper bands in Fig. 1, and the inner resonances that follow from the presence of non-standard neutrino interactions, indicated by the band at the bottom of the same figure. Here we pay special attention to the use of realistic matter and chemical supernova profiles and three-neutrino flavors thus generalising previous studies.

#### A. Neutrino Evolution in the Inner Regions

Let us first write the Hamiltonian in the inner layers, where  $H_{\text{int}} \gg H_{\text{kin}}$ . In this case the Hamiltonian can be written as

$$H \approx H_{\text{int}} = V_0 \rho (2 - Y_e) \begin{pmatrix} \frac{Y_e}{2 - Y_e} + \varepsilon_{ee} & \varepsilon_{e\mu} & \varepsilon_{e\tau} \\ \varepsilon_{e\mu} & 0 & \varepsilon_{\mu\tau} \\ \varepsilon_{e\tau} & \varepsilon_{\mu\tau} & \varepsilon_{\tau\tau} \end{pmatrix}. \quad (10)$$

When the value of the  $\varepsilon_{\alpha\beta}$  is of the same order as the electron fraction  $Y_e$  internal resonances can arise [13]. Taking into account the current constraints on the  $\varepsilon$ 's discussed in Sec. II one sees that small values of  $Y_e$  are required [46, 47]. As a result, these can only take place in the most deleptonised inner layers, close to the neutrinosphere, where the kinetic terms of the Hamiltonian are negligible.

Given the large number of free parameters  $\varepsilon_{\alpha\beta}$  involved we consider one particular case where  $|\varepsilon_{e\mu}|$  and  $|\varepsilon_{e\tau}|$  are small enough to neglect a possible initial mixing between  $\nu_e$  and  $\nu_\mu$  or  $\nu_\tau$ . Barring fine tuning, this basically amounts to  $|\varepsilon_{e\mu}|, |\varepsilon_{e\tau}| \ll 10^{-2}$ . According to the discussion of Sec. II  $\varepsilon_{e\mu}$  automatically satisfies the condition, whereas one expects that the window  $|\varepsilon_{e\tau}| \gtrsim 10^{-2}$  will eventually be probed in future experiments.

Since the initial fluxes of  $\nu_\mu$  and  $\nu_\tau$  are expected to be basically identical, it is convenient to redefine the weak basis by performing a rotation in the  $\mu - \tau$  sector:

$$\begin{pmatrix} \nu_e \\ \nu_\mu \\ \nu_\tau \end{pmatrix} = U(\vartheta'_{23}) \begin{pmatrix} \nu_e \\ \nu'_\mu \\ \nu'_\tau \end{pmatrix} = \begin{pmatrix} 1 & 0 & 0 \\ 0 & c_{23'} & s_{23'} \\ 0 & -s_{23'} & c_{23'} \end{pmatrix} \begin{pmatrix} \nu_e \\ \nu'_\mu \\ \nu'_\tau \end{pmatrix}, \quad (11)$$

where  $c_{23'}$  and  $s_{23'}$  stand for  $\cos(\vartheta'_{23})$  and  $\sin(\vartheta'_{23})$ , respectively. The angle  $\vartheta'_{23}$  can be written as

$$\tan(2\vartheta'_{23}) \approx \frac{2H_{23}}{H_{33}} = \frac{2\varepsilon_{\mu\tau}}{\varepsilon_{\tau\tau}}. \quad (12)$$

The Hamiltonian becomes in the new basis

$$\begin{aligned} H'_{\alpha\beta} &= U^\dagger(\vartheta'_{23})H_{\alpha\beta}U(\vartheta'_{23}) \\ &= V_0\rho(2 - Y_e) \begin{pmatrix} \frac{Y_e}{2-Y_e} + \varepsilon_{ee} & \varepsilon'_{e\mu} & \varepsilon'_{e\tau} \\ \varepsilon'_{e\mu} & \varepsilon'_{\mu\mu} & 0 \\ \varepsilon'_{e\tau} & 0 & \varepsilon'_{\tau\tau} \end{pmatrix}, \end{aligned} \quad (13)$$

where

$$\varepsilon'_{e\mu} = \varepsilon_{e\mu}c_{23'} - \varepsilon_{e\tau}s_{23'} \quad (15)$$

$$\varepsilon'_{e\tau} = \varepsilon_{e\mu}s_{23'} + \varepsilon_{e\tau}c_{23'} \quad (16)$$

$$\varepsilon'_{\mu\mu} = (\varepsilon_{\tau\tau} - \sqrt{\varepsilon_{\tau\tau}^2 + 4\varepsilon_{\mu\tau}^2})/2 \quad (17)$$

$$\varepsilon'_{\tau\tau} = (\varepsilon_{\tau\tau} + \sqrt{\varepsilon_{\tau\tau}^2 + 4\varepsilon_{\mu\tau}^2})/2. \quad (18)$$

With our initial assumptions on  $\varepsilon_{e\alpha}$  one notices that the new basis  $\nu'_\alpha$  basically diagonalizes the Hamiltonian, and therefore coincides roughly with the matter eigenstate basis. A novel resonance can arise if the condition  $H'_{ee} = H'_{\tau\tau}$  is satisfied, we call this *I*-resonance, *I* standing for “internal” [96]. The corresponding resonance condition can be written as

$$Y_e^I = \frac{2\varepsilon^I}{1 + \varepsilon^I}, \quad (19)$$

where  $\varepsilon^I$  is defined as  $\varepsilon'_{\tau\tau} - \varepsilon_{ee}$ . In Fig. 2 we represent the range of  $\varepsilon_{ee}$  and  $\varepsilon'_{\tau\tau}$  leading to the *I*-resonance for an electron fraction profile between different  $Y_e^{\min}$ 's and  $Y_e^{\max} = 0.5$ . It is important to notice that the value of  $Y_e^{\min}$  depends on time. Right before the collapse the minimum value of the electron fraction is around 0.4. Hence the window of NSI parameters that would lead to a resonance would be relatively narrow, as indicated by the shaded (yellow) band in Fig. 2. As time goes on  $Y_e^{\min}$  decreases to values of the order of a few %, and as a result the region of parameters giving rise to the *I*-resonance significantly widens. For example, in the range  $|\varepsilon_{ee}| \leq 10^{-3}$  possibly accessible to future experiments one sees that the *I*-resonance can take place for values of  $\varepsilon'_{\tau\tau}$  of the order of  $\mathcal{O}(10^{-2})$ . This indicates that the potential sensitivity on NSI parameters that can be achieved in supernova studies is better than that of the current limits.

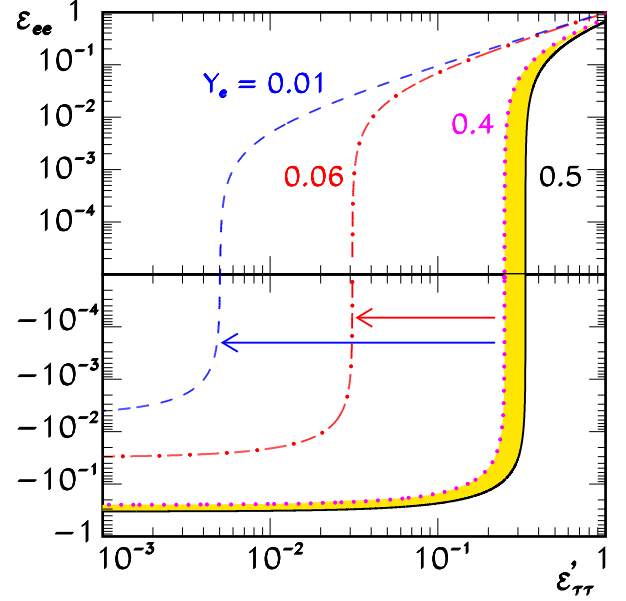


FIG. 2: Contours of  $Y_e^I$  as function of  $\varepsilon_{ee}$  and  $\varepsilon'_{\tau\tau}$  according to Eq. (19) for different values of  $Y_e$ . The region in yellow represents the region of parameters that gives rise to *I*-resonance before the collapse. The arrows indicate how this region widens with time.

As seen in Fig. 1 in order to fulfill the *I*-resonance condition for such small values of the NSI parameters the values of  $Y_e$  must indeed lie, as already stated, in the inner layers.

Several comments are in order: First, in contrast to the standard *H* and *L*-resonances, related to the kinetic term, the density itself does not explicitly enter into the resonance condition, provided that the density is high enough to neglect the kinetic terms. Analogously the energy plays no role in the resonance condition, which is determined only by the electron fraction  $Y_e$ . Moreover, in contrast to the standard resonances, the *I*-resonance occurs for both neutrinos and antineutrinos simultaneously [13]. Finally, as indicated in Fig. 3 the  $\nu_e$ 's ( $\bar{\nu}_e$ ) are not created as the heaviest (lightest) state but as the intermediate state, therefore the flavor composition of the neutrinos arriving at the *H*-resonance is exactly the opposite of the case without NSI. As we show in Sec. V, this fact can lead to important observational consequences.

In order to calculate the hopping probability between matter eigenstates at the *I*-resonance we use the Landau-

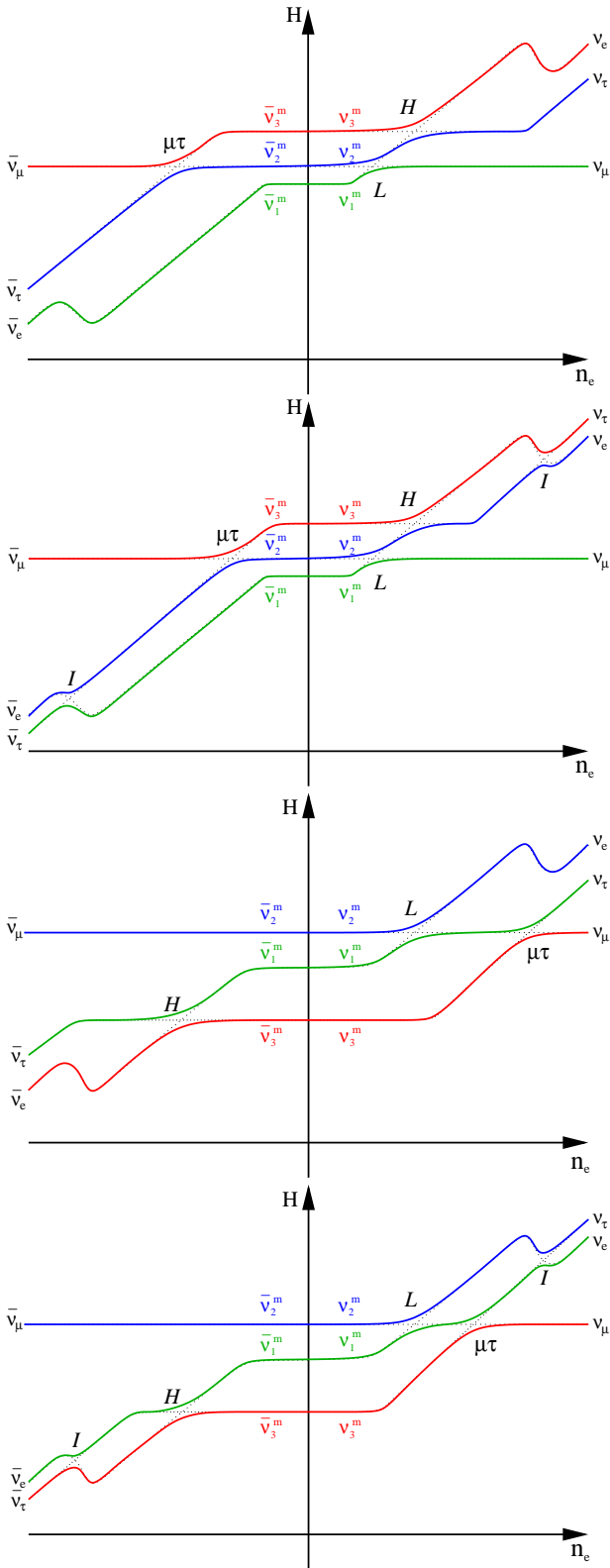


FIG. 3: Level-crossing schemes, first panel is for the case of normal hierarchy (oscillations only), the second includes the NSI effect. The two lower panels correspond to the inverse hierarchy, oscillations only and oscillations + NSI, respectively.

Zener approximation for two flavors

$$P_{LZ}^I \approx e^{-\frac{\pi}{2}\gamma_I}, \quad (20)$$

where  $\gamma_I$  stands for the adiabaticity parameter, which can be generally written as

$$\gamma_I = \left| \frac{E_2^m - E_1^m}{2\dot{\vartheta}^m} \right|_{r_I}, \quad (21)$$

where  $\dot{\vartheta}^m \equiv d\vartheta^m/dr$ . If one applies this formula to the  $e - \tau'$  box of Eq. (14) assuming that  $\tan 2\vartheta_I^m = 2H'_{e\tau}/(H'_{\tau\tau} - H_{ee})$  and  $E_2^m - E_1^m = [(H'_{\tau\tau} - H_{ee})^2 + 4H'_{e\tau}]^{1/2}$  one gets

$$\begin{aligned} \gamma_I &= \left| \frac{4H_{e\tau}'^2}{(H'_{\tau\tau} - H_{ee})} \right|_{r_I} = \left| \frac{16V_0\rho\varepsilon_{e\tau}'^2}{(1 + \varepsilon^I)^3 Y_e} \right|_{r_I} \\ &\approx 4 \times 10^9 r_{s,5} \rho_{11} \varepsilon_{e\tau}'^2 f(\varepsilon^I), \end{aligned} \quad (22)$$

where the parametrization of the  $Y_e$  profile has been defined as in Eq. (9) with  $b = 0.16$ . The density  $\rho_{11}$  represents the density in units of  $10^{11}$  g/cm<sup>3</sup>,  $r_{s,5}$  stands for  $r_s$  in units of  $10^5$  cm, and  $f(\varepsilon^I)$  is a function whose value is of the order  $\mathcal{O}(1)$  in the range of parameters we are interested in. Taking all these factors into account it follows that the internal resonance will be adiabatic provided that  $\varepsilon'_{e\tau} \gtrsim 10^{-5}$ , well below the current limits, in full numerical agreement with, e. g., Ref. [47].

In Fig. 4 we show the resonance condition as well as the adiabaticity in terms of  $\varepsilon_{\tau\tau}$  and  $\varepsilon_{e\tau}$  assuming the other  $\varepsilon_{\alpha\beta} = 0$ . In order to illustrate the dependence on time we consider profiles inspired in the numerical profiles of Fig. 1 at  $t = 2$  s (upper panel) and 15.7 s (bottom panel). For definiteness we take  $Y_e^{\min}$  as the electron fraction at which the density has value of  $5 \times 10^{11}$  g/cm<sup>3</sup>. For comparison with Fig. 2 we have assumed  $Y_e^{\min} = 10^{-2}$  in the case of 15.7 s. We observe how the border of adiabaticity depends on  $\varepsilon_{\tau\tau}$  through the value of the density at  $r_I$  which in turn depends on time.

Before moving to the discussion of the outer resonances a comment is in order, namely, how does the formalism change for other non-standard interaction models. First note that the whole treatment presented above also applies to the case of NSI on up-type quarks, except that the position of the internal resonance shifts with respect to the down-quark case. Indeed, in this case the NSI potential

$$(V_{\text{nsi}}^u)_{\alpha\beta} = \varepsilon_{\alpha\beta}^u V_0 \rho (1 + Y_e), \quad (23)$$



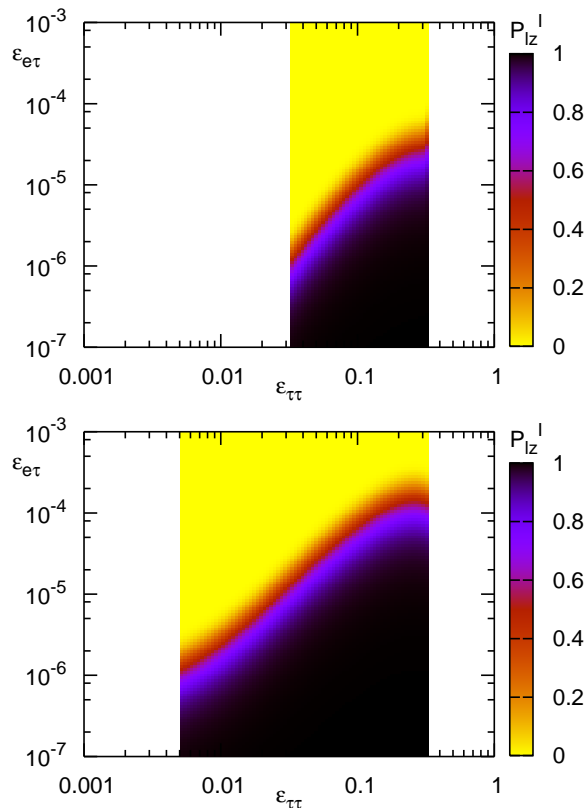


FIG. 4: Contours of constant jump probability at the  $I$ -resonance in terms of  $\varepsilon_{\tau\tau}$  and  $\varepsilon_{e\tau}$  for two profiles corresponding to Fig. 1 at 2 s with  $a = 0.235$  and  $b = 0.175$  (upper panel) and 15.7 s with  $a = 0.26$  and  $b = 0.195$  (bottom panel). For simplicity the other  $\varepsilon$ 's have been set to zero.

would induce a similar internal resonance for the condition  $Y_e = \varepsilon^I/(1 - \varepsilon^I)$ .

In contrast, for the case of NSI with electrons, the NSI potential is proportional to the electron fraction, and therefore no internal resonance would appear.

### B. Neutrino Evolution in the Outer Regions

In the outer layers of the SN envelope neutrinos can undergo important flavor transitions at those points where the matter induced potential equals the kinetic terms. In absence of NSI this condition can be expressed as  $V_{CC} \approx \Delta m^2/(2E)$ . Neutrino oscillation experiments indicate two mass scales,  $\Delta m_{\text{atm}}^2$  and  $\Delta m_{\odot}^2 \equiv m_2^2 - m_1^2$  [5], hence two different resonance layers arise, the so-called  $H$ -resonance and the  $L$ -resonance, respectively.

The presence of NSI with values of  $|\varepsilon_{\alpha\beta}| \lesssim 10^{-2}$  modi-

fies the properties of the  $H$  and  $L$  transitions [48, 49, 50]. In particular one finds that the effects of the NSI can be described as in the standard case by embedding the  $\varepsilon$ 's into effective mixing angles [50]. An analogous ‘‘confusion’’ between  $\sin \vartheta_{13}$  and the corresponding NSI parameter  $\varepsilon_{e\tau}$  has been pointed out in the context of long-baseline neutrino oscillations in Refs. [53, 54].

In this section we perform a more general and complementary study for slightly higher values of the NSI parameters:  $|\varepsilon_{\alpha\beta}| \gtrsim \text{few } 10^{-2}$ , still allowed by current limits, and for which the  $I$ -resonance could occur.

The phenomenological assumption of hierarchical squared mass differences,  $|\Delta m_{\text{atm}}^2| \gg \Delta m_{\odot}^2$ , allows, for not too large  $\varepsilon$ 's, a factorization of the  $3\nu$  dynamics into two  $2\nu$  subsystems roughly decoupled for the  $H$  and  $L$  transitions [65]. To isolate the dynamics of the  $H$  transition, one usually rotates the neutrino flavor basis by  $U^\dagger(\vartheta_{23})$ , and extracts the submatrix with indices (1,3) [48, 50]. Whereas this method works perfectly for small values of  $\varepsilon_{\alpha\beta}$  it can be dangerous for values above  $10^{-2}$ . In order to analyze how much our case deviates from the simplest approximation we have performed a rotation with the angle  $\vartheta_{23}'' \equiv \vartheta_{23} - \alpha$  instead of just  $\vartheta_{23}$ . By requiring that the new rotation diagonalizes the submatrix (2,3) at the  $H$ -resonance layer one obtains the following expression for the correction angle  $\alpha$

$$\tan(2\alpha) = \frac{[\Delta_{\odot} s_{212} s_{13} + V_{\tau\tau}^{\text{NSI}} s_{223} - 2V_{\mu\tau}^{\text{NSI}} c_{223}]}{\left[ (\Delta_{\text{atm}} + \frac{1}{2}\Delta_{\odot}) c_{13}^2 + \frac{1}{4}\Delta_{\odot} c_{212}(-3 + c_{213}) + V_{\tau\tau}^{\text{NSI}} c_{223} + 2V_{\mu\tau}^{\text{NSI}} s_{223} \right]}, \quad (24)$$

where  $\Delta_{\text{atm}} \equiv \Delta m_{\text{atm}}^2/(2E)$  and  $\Delta_{\odot} \equiv \Delta m_{\odot}^2/(2E)$ . In our notation  $s_{ij}$  and  $s_{2ij}$  represent  $\sin \vartheta_{ij}$  and  $\sin(2\vartheta_{ij})$ , respectively. The parameters  $c_{ij}$  and  $c_{2ij}$  are analogously defined. In the absence of NSI  $\alpha$  is just a small correction to  $\vartheta_{23}$  [97],

$$\tan(2\alpha) \approx \Delta_{\odot} s_{212} s_{13} / \Delta_{\text{atm}} c_{13}^2 \lesssim \mathcal{O}(10^{-3}). \quad (25)$$

In order to calculate  $\alpha$  we need to know the  $H$ -resonance point. To calculate it one can proceed as in the case without NSI, namely, make the  $\vartheta_{23}''$  rotation and analyze the submatrix (1,3). The new Hamiltonian  $H''_{\alpha\beta}$  has now the form

$$H''_{ee} = V_0 \rho [Y_e + \varepsilon_{ee}(2 - Y_e)] + \Delta_{\text{atm}} s_{13}^2$$

$$\begin{aligned}
& +\Delta_{\odot}(c_{13}^2s_{12}^2 + s_{13}^2) , \\
H''_{\tau\tau} &= V_0\rho(2 - Y_e)\varepsilon''_{\tau\tau} + \Delta_{\text{atm}}c_{13}^2c_{\alpha}^2 \\
& +\Delta_{\odot} [c_{13}^2c_{\alpha}^2 + (s_{\alpha}c_{12} + c_{\alpha}s_{12}s_{13})^2] , \\
H''_{e\tau} &= V_0\rho(2 - Y_e)\varepsilon''_{e\tau} + \frac{1}{2}\Delta_{\text{atm}}s_{213}c_{\alpha} \\
& +\frac{1}{2}\Delta_{\odot}(-c_{13}s_{\alpha}s_{212} + c_{12}^2c_{\alpha}s_{213}) . \quad (26)
\end{aligned}$$

We have defined  $\varepsilon''_{\tau\tau} = \varepsilon_{\tau\tau}c_{23-\alpha}^2 + \varepsilon_{\mu\tau}s_{23-\alpha}$ , and  $\varepsilon''_{e\tau} = \varepsilon_{e\tau}c_{23-\alpha} + \varepsilon_{e\mu}s_{23-\alpha}$ , where  $s_{23-\alpha} \equiv \sin(\vartheta_{23}-\alpha)$ ,  $c_{23-\alpha} \equiv \cos(\vartheta_{23}-\alpha)$ , and  $s_{2\vartheta_{23}-2\alpha} \equiv \sin(2\vartheta_{23}-2\alpha)$ ,  $c_{2\vartheta_{23}-2\alpha} \equiv \cos(2\vartheta_{23}-2\alpha)$ . The resonance condition for the  $H$  transition,  $H''_{ee} = H''_{\tau\tau}$  can be then written as

$$\begin{aligned}
V_0\rho^H [Y_e^H + (\varepsilon_{ee} - \varepsilon''_{\tau\tau})(2 - Y_e^H)] &= \Delta_{\text{atm}}(c_{13}^2c_{\alpha}^2 - s_{13}^2) \\
& +\Delta_{\odot}[c_{12}^2(c_{13}^2 - c_{\alpha}^2s_{13}^2) - s_{\alpha}^2s_{12}^2 + \frac{1}{2}s_{2\alpha}s_{212}s_{13}] \quad (27)
\end{aligned}$$

It can be easily checked how in the limit of  $\varepsilon_{\alpha\beta} \rightarrow 0$  one recovers the standard resonance condition,

$$V_0\rho^HY_e^H \approx \Delta_{\text{atm}}c_{213} . \quad (28)$$

In the region where the  $H$ -resonance occurs  $Y_e^H \approx 0.5$ .

Taking into account Eqs. (24) and (27) one can already estimate how the value of  $\alpha$  changes with the NSI parameters. In Fig. 5 we show the dependence of  $\alpha$  on the  $\varepsilon_{\tau\tau}$  after fixing the value of the other NSI parameters. One can see how for  $\varepsilon_{\tau\tau} \gtrsim 10^{-2}$  the approximation of neglecting  $\alpha$  significantly worsens. Assuming  $\vartheta_{23} = \pi/4$  and a fixed value of  $\varepsilon_{\mu\tau}$  one can easily see that  $\varepsilon_{\tau\tau}$  basically affects the numerator in Eq. (24). Therefore one expects a rise of  $\alpha$  as the value of  $\varepsilon_{\tau\tau}$  increases, as seen in Fig. 5. The dependence of  $\alpha$  on  $\varepsilon_{\mu\tau}$  is correlated to the relative sign of the mass hierarchy and  $\varepsilon_{\mu\tau}$ . For instance, for normal mass hierarchy and positive values of  $\varepsilon_{\mu\tau}$  the dependence is inverse, namely, higher values of  $\varepsilon_{\mu\tau}$  lead to a suppression of  $\alpha$ . Apart from this general behavior,  $\alpha$  also depends on the diagonal term  $\varepsilon_{ee}$  as seen in Fig. 5. This effect occurs by shifting the resonance point through the resonance condition in Eq. (27).

One can now calculate the jump probability between matter eigenstates in analogy to the  $I$ -resonance by means of the Landau-Zener approximation, see Eqs. (20), (21), and 22,

$$P_{LZ}^H \approx e^{-\frac{\pi}{2}\gamma_H} , \quad (29)$$

where  $\gamma_H$  represents the adiabaticity parameter at the

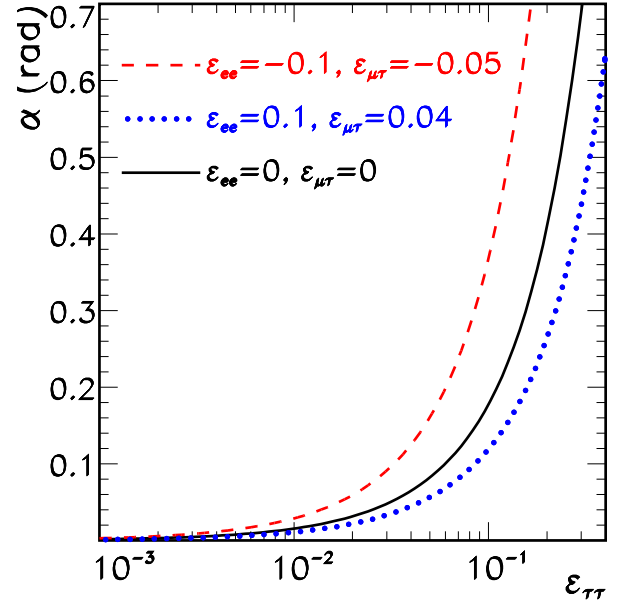


FIG. 5: Angle  $\alpha$  as function of  $\varepsilon_{\tau\tau}$  for different values of  $\varepsilon_{ee}$  and  $\varepsilon_{\mu\tau}$ , in the case of neutrinos of energy 10 MeV, with normal mass hierarchy, and  $s_{13}^2 = 10^{-5}$ . The other NSI parameters take the following values:  $\varepsilon_{e\mu} = 0$  and  $\varepsilon_{e\tau} = 10^{-3}$ .

$H$ -resonance, which can be written as

$$\gamma_H = \left| \frac{4H''_{e\tau}}{(\dot{H}''_{\tau\tau} - \dot{H}''_{ee})} \right|_{r_H} , \quad (30)$$

where the expressions for  $H''_{\alpha\beta}$  are given in Eqs (26).

Let us first consider the case  $|\varepsilon_{\alpha\beta}| \lesssim 10^{-2}$ . In this case  $\alpha \approx 0$  and one can rewrite the adiabaticity parameter as

$$\gamma_H \approx \frac{\Delta_{\text{atm}} \sin^2(2\vartheta_{13}^{\text{eff}})}{\cos(2\vartheta_{13}^{\text{eff}}) |d \ln V / dr|_{r_H}} , \quad (31)$$

where

$$\vartheta_{13}^{\text{eff}} = \vartheta_{13} + \varepsilon''_{e\tau}(2 - Y_e)/Y_e \quad (32)$$

in agreement with Ref. [50]. For slightly larger  $\varepsilon$ 's there can be significant differences. In Fig. 6 we show  $P_{LZ}^H$  in the  $\varepsilon_{e\tau}$ - $\varepsilon_{\tau\tau}$  plane for antineutrinos with energy 10 MeV in the case of inverse mass hierarchy, using Eq. (29) with (upper panel) and without (bottom panel) the  $\alpha$  correction. The values of  $\vartheta_{13}$  and  $\varepsilon_{e\tau}$  have been chosen so that the jump probability lies in the transition regime between adiabatic and strongly non adiabatic. In the limit of small  $\varepsilon_{\tau\tau}$ ,  $\alpha$  becomes negligible and therefore both results coincide. From Eq. (31) one sees how as the value of

$\varepsilon_{e\tau}$  increases  $\gamma_H$  gets larger and therefore the transition becomes more and more adiabatic. For negative values of  $\varepsilon_{e\tau}$  there can be a cancellation between  $\varepsilon_{e\tau}$  and  $\vartheta_{13}$ , and as a result the transition becomes non-adiabatic.

An additional consequence of Eq. (32) is that a degeneracy between  $\varepsilon_{e\tau}$  and  $\vartheta_{13}$  arises. This is seen in Fig. 7, which gives the contours of  $P_{LZ}^H$  in terms of  $\varepsilon_{e\tau}$  and  $\vartheta_{13}$  for  $\varepsilon_{\tau\tau} = 10^{-4}$ . One sees clearly that the same Landau-Zener hopping probability is obtained for different combinations of  $\varepsilon_{e\tau}$  and  $\vartheta_{13}$ . This leads to an intrinsic ‘‘confusion’’ between the mixing angle and the corresponding NSI parameter, which can not be disentangled only in the context of SN neutrinos, as noted in Ref. [50].

We now turn to the case of  $|\varepsilon_{\tau\tau}| \geq 10^{-2}$ . As  $|\varepsilon_{\tau\tau}|$  increases the role of  $\alpha$  becomes relevant. Whereas in the bottom panel  $P_{LZ}^H$  remains basically independent of  $\varepsilon_{\tau\tau}$ , one can see how in the upper panel  $P_{LZ}^H$  becomes strongly sensitive to  $\varepsilon_{\tau\tau}$  for  $|\varepsilon_{\tau\tau}| \geq 10^{-2}$ .

One sees that for positive values of  $\varepsilon_{\tau\tau}$  it tends to adiabaticity whereas for negative values to non-adiabaticity. This follows from the dependence of  $H''_{e\tau}$  on  $\alpha$ , essentially through the term  $-\Delta_{\odot} c_{13} s_{\alpha} s_{212}$ , see Eq. (26). For  $|\varepsilon_{\tau\tau}| \geq 10^{-2}$  one sees that  $\sin \alpha$  starts being important, and as a result this term eventually becomes of the same order as the others in  $H''_{e\tau}$ . At this point the sign of  $\varepsilon_{\tau\tau}$ , and so the sign of  $\sin \alpha$ , is crucial since it may contribute to the enhancement or reduction of  $H''_{e\tau}$ . This directly translates into a trend towards adiabaticity or non-adiabaticity, seen in Fig. 6. Thus, for the range of  $\varepsilon_{\tau\tau}$  relevant for the NSI-induced internal resonance the adiabaticity of the outer  $H$  resonance can be affected in a non-trivial way.

Turning to the case of the  $L$  transition a similar expression can be obtained by rotating the original Hamiltonian by  $U(\vartheta_{13})^{\dagger} U(\vartheta_{23})^{\dagger}$  [48, 50]. However, in contrast to the case of the  $H$ -resonance, where the mixing angle  $\vartheta_{13}$  is still unknown, in the case of the  $L$  transition the angle  $\vartheta_{12}$  has been shown by solar and reactor neutrino experiments to be large [5]. As a result, for the mass scale  $\Delta_{\odot}$  this transition will always be adiabatic irrespective of the values of  $\varepsilon_{\alpha\beta}$ , and will affect only neutrinos.

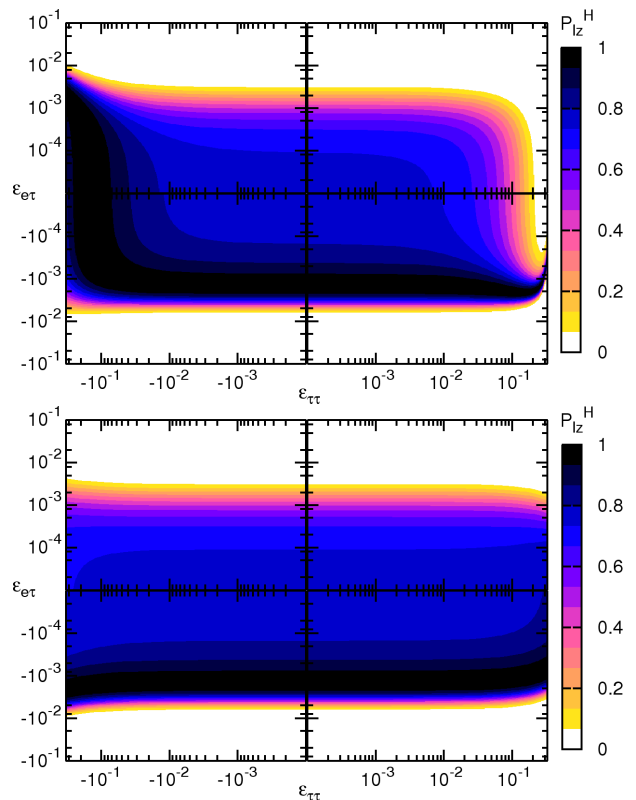


FIG. 6: Landau-Zener jump probability isocontours at the  $H$ -resonance in terms of  $\varepsilon_{e\tau}$  and  $\varepsilon_{\tau\tau}$  for 10 MeV antineutrinos in the case of inverted mass hierarchy. Upper panel:  $\alpha$  given by Eq. (24). Bottom panel:  $\alpha$  set to zero. The remaining parameters take the following values:  $\sin^2 \vartheta_{13} = 10^{-5}$ ,  $\varepsilon_{e\tau} = 10^{-3}$ ,  $\varepsilon_{ee} = \varepsilon_{e\mu} = 0$ . See text.

## V. OBSERVABLES AND SENSITIVITY

As mentioned in the introduction one of the major motivations to study NSI using the neutrinos emitted in a SN is the enhancement of the NSI effects on the neutrino propagation through the SN envelope due to the specific extreme matter conditions that characterize it. In this section we analyze how these effects translate into observable effects in the case of a future galactic SN.

Schematically, the neutrino emission by a SN can be divided into four stages: Infall phase, neutronization burst, accretion, and Kelvin-Helmholtz cooling phase. During the infall phase and neutronization burst only  $\nu_e$ 's are emitted, while the bulk of neutrino emission is released in all flavors in the last two phases. Whereas the neutrino emission characteristics of the two initial stages are basi-

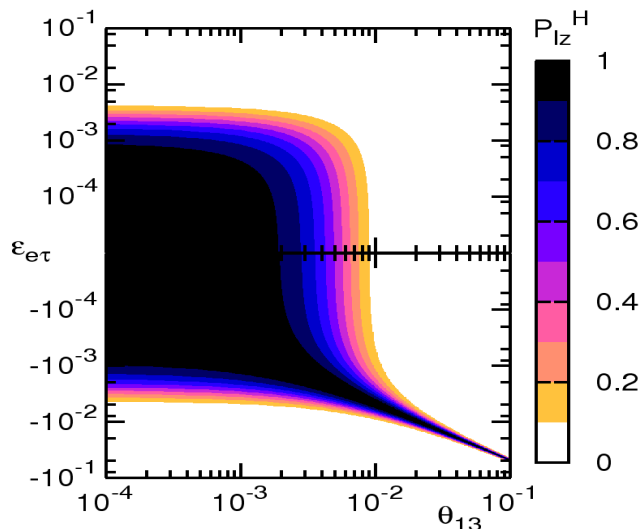


FIG. 7: Landau-Zener jump probability isocontours at the  $H$ -resonance in terms of  $\epsilon_{e\tau}$  and  $\theta_{13}$  for  $\epsilon_{\tau\tau} = 10^{-4}$ . Antineutrinos with energy 10 MeV and inverted mass hierarchy has been assumed.

cally independent of the features of the progenitor, such as the core mass or equation of state (EoS), the details of the neutrino spectra and luminosity during the accretion and cooling phases may significantly change for different progenitor models. As a result, a straightforward extraction of oscillation parameters from the bulk of the SN neutrino signal seems hopeless. Only features in the detected neutrino spectra which are independent of unknown SN parameters should be used in such an analysis [66].

The question then arises as to how can one obtain information about the NSI parameters. Taking into account that the main effect of NSI is to generate new internal neutrino flavor transitions, one possibility is to invoke theoretical arguments that involve different aspects of the SN internal dynamics.

In Ref. [47] it was argued that such an internal flavor conversion during the first second after the core bounce might play a positive role in the so-called SN shock re-heating problem. It is observed in numerical simulations [67, 68, 69, 70] that as the shock wave propagates it loses energy until it gets stalled at a few hundred km. It is currently believed that after neutrinos escape the SN core they can to some extent deposit energy right behind and help the shock wave continue out-

wards. On the other hand it is also believed that due to the composition in matter of the protoneutronstar (PNS) the mean energies of the different neutrino spectra obey  $\langle E_{\nu_e} \rangle < \langle E_{\bar{\nu}_e} \rangle < \langle E_{\nu_\mu, \nu_\tau} \rangle$ . This means that a resonant conversion between  $\nu_e(\bar{\nu}_e)$  and  $\nu_{\mu, \tau}(\bar{\nu}_{\mu, \tau})$  between the neutrinosphere and the position of the stalled shock wave would make the  $\nu_e(\bar{\nu}_e)$  spectra harder, and therefore the energy deposition would be larger, giving rise to a shock wave regeneration effect.

Another argument used in the literature was the possibility that the  $r$ -process nucleosynthesis, responsible for synthesizing about half of the heavy elements with mass number  $A > 70$  in nature, could occur in the region above the neutrinosphere in SNe [71, 72]. A necessary condition is  $Y_e < 0.5$  in the nucleosynthesis region. The value of the electron fraction depends on the neutrino absorption rates, which are determined in turn by the  $\nu_e(\bar{\nu}_e)$  luminosities and energy distribution. These can be altered by flavor conversion in the inner layers due to the presence of NSI. Therefore by requiring the electron fraction be below 0.5 one can get information about the values of the NSI parameters.

While it is commonly accepted that neutrinos will play a crucial role in both the shock wave re-heating as well as the  $r$ -process nucleosynthesis, there are still other astrophysical factors that can affect both. While the issue remains under debate we prefer to stick to arguments directly related to physical observables in a large water Cherenkov detector. There are several possibilities.

- (A) the modulations in the  $\bar{\nu}_e$  spectra due to the passage of shock waves through the supernova [58, 59, 60]
- (B) the modulation in the  $\bar{\nu}_e$  spectra due to the time dependence of the electron fraction, induced by the  $I$ -resonance
- (C) the modulations in the  $\bar{\nu}_e$  spectra due to the Earth matter [73, 74, 75, 76]
- (D) detectability of the neutronization  $\nu_e$  burst [77, 78]

Three of these observables, 1, 3 and 4 have already been considered in the literature in the context of neutrino oscillations. Here we discuss the potential of the above promising observables in providing information about the

Scheme	Hierarchy	$\sin^2 \vartheta_{13}$	NSI	$P_{\text{surv}}$	$\bar{P}_{\text{surv}}$
<i>A</i>	normal	$\gtrsim 10^{-4}$	No	0	$\cos^2 \vartheta_{12}$
<i>B</i>	inverted	$\gtrsim 10^{-4}$	No	$\sin^2 \vartheta_{12}$	0
<i>C</i>	any	$\lesssim 10^{-6}$	No	$\sin^2 \vartheta_{12}$	$\cos^2 \vartheta_{12}$
<i>AI</i>	normal	$\gtrsim 10^{-4}$	Yes	$\sin^2 \vartheta_{12}$	$\sin^2 \vartheta_{12}$
<i>BI</i>	inverted	$\gtrsim 10^{-4}$	Yes	$\cos^2 \vartheta_{12}$	$\cos^2 \vartheta_{12}$
<i>CIa</i>	normal	$\lesssim 10^{-6}$	Yes	0	$\sin^2 \vartheta_{12}$
<i>CIb</i>	inverted	$\lesssim 10^{-6}$	Yes	$\cos^2 \vartheta_{12}$	0

TABLE I: Definition of the neutrino schemes considered in terms of the hierarchy, the value of  $\vartheta_{13}$ , and the presence of NSI, as described in the text. The values of the survival probabilities for  $\nu_e$  ( $P_{\text{surv}}$ ) and  $\bar{\nu}_e$  ( $\bar{P}_{\text{surv}}$ ) for each case are also indicated.

NSI parameters. It is important to pay attention to the possible occurrence of the internal *I*-resonance and to its effect in the external *H* and *L*-resonances. The first can induce a genuinely new observable effect, item 2 above.

Here we concentrate on neutral current-type non-standard interactions, hence there will be not effect in the main reaction in water Cherenkov and scintillator detectors, namely the inverse beta decay,  $\bar{\nu}_e + p \rightarrow e^+ + n$  [98]. For definiteness we take NSI with *d* (down) quarks, in which case the NSI effects will be confined to the neutrino evolution inside the SN and the Earth, through the vector component of the interaction.

From all possible combinations of NSI parameters we will concentrate on those for which the internal *I* transition does take place, namely  $|\varepsilon^I| \gtrsim 10^{-2}$ , see Fig. 2. Concerning the FC NSI parameters we will consider  $|\varepsilon'_{e\tau}|$  between  $\text{few} \times 10^{-5}$  and  $10^{-2}$ , range in which the *I*-resonance is adiabatic, see Fig. 4. In the following discussion we will focus on the extreme cases defined in Table I. One of the motivations for considering these cases is the fact that the resonances involved become either adiabatic or strongly non adiabatic, and hence the survival probabilities in the absence of Earth effects or shock wave passage, become energy independent. This assumption simplifies the task of relating the observables with the neutrino schemes.

## A. Shock wave propagation

During approximately the first two seconds after the core bounce, the neutrino survival probabilities are constant in time and in energy for all cases mentioned in Table I. Only the Earth effects could introduce an energy dependence. However, at  $t \approx 2$  s the *H*-resonance layer is reached by the outgoing shock wave, see Fig. 1. The way the shock wave passage affects the neutrino propagation strongly depends on the neutrino mixing scenario. In the absence of NSI cases *A* and *C* will not show any evidence of shock wave propagation in the observed  $\bar{\nu}_e$  spectrum, either because there is no resonance in the antineutrino channel as in scenario *A*, or because the *H*-resonance is always strongly non-adiabatic as in scenario *C*. However, in scenario *B*, the sudden change in density breaks the adiabaticity of the resonance, leading to a time and energy dependence of the electron antineutrino survival probability  $\bar{P}_{\text{surv}}(E, t)$ . In the upper panel of Fig. 8 we show  $\bar{P}_{\text{surv}}(E, t)$  in the particular case that two shock waves are present, one forward and a reverse one [60]. The presence of the shocks results in the appearance of bumps in survival probability at those energies for which the resonance region is passed by the shock waves. All these structures move in time towards higher energies, as the shock waves reach regions with lower density, leading to observable consequences in the  $\bar{\nu}_e$  spectrum.

We now turn to the case where NSI are present, which opens the possibility of internal resonances. When such *I*-resonance is adiabatic the situation will be similar to the case without NSI. For normal mass hierarchy, *AI* and *CIa*,  $\bar{\nu}_e$  will not feel the *H*-resonance and therefore the adiabaticity-breaking effect will not basically alter their propagation. In contrast, for inverted mass hierarchy and large  $\vartheta_{13}$ , case *BI*, the *H*-resonance occurs in the antineutrino channel and therefore  $\bar{\nu}_e$  will feel the shock wave passage. However, in contrast to case *B* now  $\bar{\nu}_e$  will reach the *H*-resonance in a different matter eigenstate:  $\bar{\nu}_1^m$  instead of  $\bar{\nu}_3^m$ , see Fig. 3. That means that before the shock wave reaches the *H*-resonance the  $\bar{\nu}_e$  survival probability will be  $\bar{P}_{\text{surv}} \approx \cos^2 \vartheta_{12} \approx 0.7$ . Once the adiabaticity of the *H*-resonance is broken by the shock wave then  $\bar{\nu}_e$  will partly leave as  $\bar{\nu}_3^m$  and therefore the survival probability will decrease. As a consequence one expects a pattern in time and energy for the survival

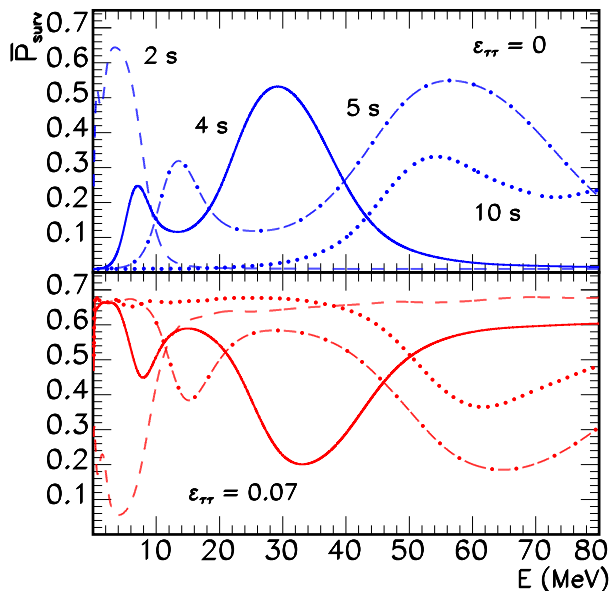


FIG. 8: Survival probability  $\bar{P}_{\text{surv}}(E, t)$  for  $\bar{\nu}_e$  as function of energy at different times averaged in energies with the energy resolution of Super-Kamiokande; for the profile shown in Fig. 1. Upper panel: case *B* is assumed for  $\sin^2 \vartheta_{13} = 10^{-2}$ . Bottom panel: case *BI*, with  $\varepsilon_{\tau\tau} = 0.07$ ,  $\varepsilon_{e\tau} = 10^{-4}$  and the rest of NSI parameters put to zero.

probability in the case *BI* to be roughly *opposite* than in the case *B*, see bottom panel of Fig. 8. The position of the peaks and dips in each panel do not exactly coincide as the value of  $\varepsilon_{\tau\tau}$  roughly shifts the position of the *H*-resonance.

In the left panels of Fig. 9 we represent in light-shaded (yellow) the range of  $\varepsilon_{e\tau}$  and  $\varepsilon_{\tau\tau}$  for which this *opposite* shock wave imprint would be observable. In the upper panels we have assumed a minimum value of the electron fraction of 0.06, based on the numerical profiles at  $t = 2$  s of Fig. 1. In the bottom panels  $Y_e^{\text{min}}$  is set to 0.01, inspired in the profiles at  $t = 15.7$  s. It can be seen how as time goes on the range of  $\varepsilon_{\tau\tau}$ 's for which the *I*-resonance takes place widens towards to smaller and smaller values. This is a direct consequence of the steady deleptonization of the inner layers.

For smaller  $\vartheta_{13}$ , case *CIb*, the situation is different. Except for relatively large  $\varepsilon_{e\tau}$  values the *H*-resonance will be strongly non-adiabatic, as in case *C*. Therefore the passage of the shock waves will not significantly change the  $\bar{\nu}_e$  survival probability and will not lead to any ob-

servable effect. In the right panels of Fig. 9 we show the same as in the left panels but for  $\sin^2 \vartheta_{13} = 10^{-7}$ . Whereas for large values of  $\vartheta_{13}$ , left panels, the *H*-resonance is always adiabatic and one has only to ensure the adiabaticity of the *I*-resonance, for smaller values of  $\vartheta_{13}$  the adiabaticity of the *H*-resonance strongly depends on the values of  $\varepsilon_{e\tau}$  and  $\varepsilon_{\tau\tau}$ , as discussed in Sec. IV B. This can be seen as a significant reduction of the yellow area. Only large values of either  $\varepsilon_{e\tau}$  or  $\varepsilon_{\tau\tau}$  would still allow for a clear identification of the *opposite* shock wave effects. In dark-shaded (cyan) we show the region of parameters for which  $P_H$  lies in the transition region between adiabatic and strongly non-adiabatic, and therefore could still lead to some effect.

A useful observable to detect effects of the shock propagation is the average of the measured positron energies,  $\langle E_e \rangle$ , produced in inverse beta decays. In Fig. 10, we show  $\langle E_e \rangle$  together with the one sigma errors expected for a Megaton water Cherenkov detector and a SN at 10 kpc distance, with a time binning of 0.5 s, for different neutrino schemes: case *B* and case *BI* with different values of  $\varepsilon_{\tau\tau}$ . For the neutrino fluxes we assumed the parametrization given by Refs. [79, 80] with  $\langle E_0(\bar{\nu}_e) \rangle = 15$  MeV and  $\langle E_0(\bar{\nu}_{\mu,\tau}) \rangle = 18$  MeV and the following ratio of the total neutrino fluxes  $\Phi_0(\bar{\nu}_e)/\Phi_0(\bar{\nu}_{\mu,\tau}) = 0.8$  [99].

One can see how the features of the average positron energy are a direct consequence of the shape of the survival probability, where dips have to be translated into bumps and vice-versa.

Thus, it is important to stress that whereas in case *B* one expects the presence of one or two dips (depending on the structure of the shock wave, see Ref [60]), or nothing in the other cases, one or two bumps are expected in case *BI*, as seen in the upper left panel of Fig. 10. As discussed in Ref. [60] the details of the dips/bump will depend on the exact shape of the neutrino fluxes, but as long as general reasonable assumptions like  $\langle E_{\bar{\nu}_e} \rangle \lesssim \langle E_{\bar{\nu}_{\mu,\tau}} \rangle$  are considered the dips/bumps should be observed.

## B. Time variation of $Y_e$

We have just seen how the distortion of the density profile due to the shock wave passage through the outer

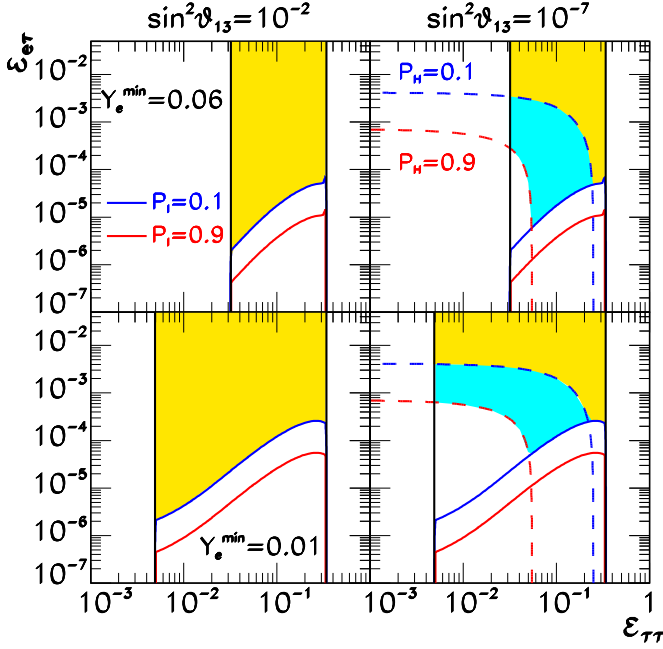


FIG. 9: Range of  $\varepsilon_{\tau\tau}$  and  $\varepsilon_{e\tau}$  for which the effect of the shock wave will be observed. In the upper panels a minimum value of  $Y_e^{\min} = 0.06$  based on the numerical profiles at  $t = 2$  s has been assumed, see Fig. 1. In the lower panels we have considered a case with  $Y_e^{\min} = 0.01$  inspired in the profile at  $t = 15.7$  s. The value of  $\sin^2 \vartheta_{13}$  has been assumed to be  $10^{-2}$  and  $10^{-7}$  in the left and right panels, respectively. We have also superimposed isocontours of constant hopping probability 0.1 (blue) and 0.9 (red) in the  $I$  (solid lines) and  $H$  (dashed lines) resonances for inverted mass hierarchy and  $E = 10$  MeV and antineutrinos. The area in yellow represents the parameter space where both resonances will be adiabatic. In the cyan area the  $I$ -resonance is assumed to be adiabatic whereas  $H$  lies in the transition region.

SN envelope can induce a time-dependent modulation in the  $\bar{\nu}_e$  spectrum in cases  $B$  and  $BI$ . However the time dependence of the electron fraction  $Y_e$  can also reveal the presence of NSI leaving a clear imprint in the observed  $\bar{\nu}_e$  spectrum, as we now explain.

As discussed in Sec. IV A the region of NSI parameters leading to  $I$ -resonance is basically determined by the minimum and maximum values of the electron fraction,  $Y_e^{\min}$  and  $Y_e^{\max}$ . The crucial point is that as the deleptonization of the proto-neutron star goes on, the value of  $Y_e^{\min}$  steadily decreases with time. As a result, the range of NSI strengths for which the  $I$ -resonance takes place

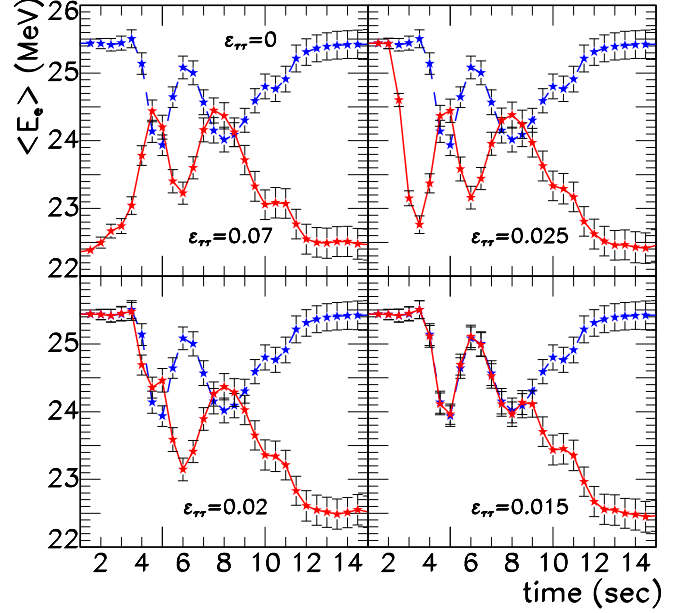


FIG. 10: The average energy of  $\bar{\nu}p \rightarrow ne^+$  events binned in time for case  $B$  (dashed blue) and  $BI$  (solid red). In each panel different values of  $\varepsilon_{\tau\tau}$  have been assumed. The error bars represent  $1\sigma$  errors in any bin.  $\varepsilon_{e\tau} = 10^{-4}$ .

increases with time, as can be seen in Fig. 2.

Let us first discuss the observational consequences of the time dependence of the electron fraction in case  $BI$ . If  $\varepsilon_{\tau\tau}$  ( $\varepsilon^I$  in general) is large enough the  $I$ -resonance will take place right after the core bounce. In this case, as seen in the upper left panel of Fig. 10 the two bumps we have just discussed in Sec. V A would be clearly observed. However for smaller NSI parameter values it could happen that the  $I$ -resonance occurs only after several seconds. In particular for the specific  $Y_e$  profile considered we show how this delay could be of roughly 2, 4 or 9 sec for values of  $\varepsilon_{\tau\tau}$  of 0.025, 0.02 or 0.015, respectively, see last three panels Fig. 10. As can be inferred from the figure this delay effect can lead to misidentification of the pure NSI effect. So, for instance, in the upper right panel, one sees how the two bumps might also be interpreted as two dips, given the astrophysical uncertainties. This subtle degeneracy can only be solved by extra information on, for example, the time dependence of the spectra or the velocity of the shock wave. Given the supernova model, however, the time structure of the signal

could eventually not only point out the presence of NSI but even potentially indicate a range of NSI parameters.

Let us now turn to the normal mass hierarchy scenario (cases *AI* and *CIa*). In analogy to the *BI* case, if  $\varepsilon^I$  is relatively large the onset of the *I*-resonance will take place early on. As can be inferred from Fig. 3 that implies that  $\bar{\nu}_e$  will escape the SN as  $\bar{\nu}_2$ . For smaller values, though, it may happen that the *I*-resonance becomes effective only after a few seconds. This means that during the first seconds of the neutrino signal  $\bar{\nu}_e$  would leave the star as  $\bar{\nu}_1$  (cases *A* and *C*). Then, after some point, the electron fraction would be low enough to switch on the *I*-resonance, and consequently  $\bar{\nu}_e$  would enter the Earth as  $\bar{\nu}_2$ . This would result in a transition in the electron antineutrino survival probability from  $\bar{P}_{\text{surv}} \approx \cos^2 \vartheta_{12} = 0.7$  to  $\sin^2 \vartheta_{12} = 0.3$ . Given the expected hierarchy in the average neutrino energies  $\langle E_{\bar{\nu}_e} \rangle \lesssim \langle E_{\bar{\nu}_{\mu,\tau}} \rangle$ , it follows that the change in  $Y_e$  would lead to a hardening of the observed positron spectrum. The effect is quantified in Fig. 11 for different values of  $\varepsilon_{\tau\tau}$ . The figure shows the average energy of the  $\bar{\nu}p \rightarrow ne^+$  events for the case of a Megaton water Cherenkov detector exactly as in Fig. 10, but for scenarios *AI* and *CIa*. One can see how for  $\varepsilon_{\tau\tau} = 0.07$  the *I*-resonance condition is always fulfilled and therefore there is no time dependence. However for smaller values one can see a rise at a certain moment which depends on the magnitude of  $\varepsilon_{\tau\tau}$ . A similar effect would occur in case *CIb*.

### C. Earth matter effects

Before the shock wave reaches the *H*-resonance layer the dependence of the neutrino survival probability in the cases we are considering, on the neutrino energy  $E$  is very weak. However, if neutrinos cross the Earth before reaching the detector, the conversion probabilities may become energy-dependent, inducing modulations in the neutrino energy spectrum. These modulations may be observed in the form of local peaks and valleys in the spectrum of the event rate  $\sigma F_{\bar{\nu}_e}^D$  plotted as a function of  $1/E$ . These modulations arise in the antineutrino channel only when  $\bar{\nu}_e$  leave the SN as  $\bar{\nu}_1$  or  $\bar{\nu}_2$ . In the absence of NSI this happens in cases *A* and *C*, where  $\bar{\nu}_e$  leave the star as  $\bar{\nu}_1$ .

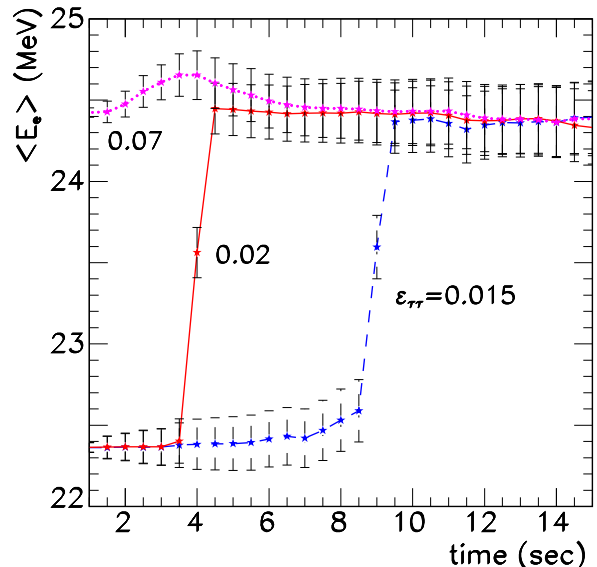


FIG. 11: The average energy of  $\bar{\nu}p \rightarrow ne^+$  events binned in time for case *AI* and *CIa* and different values of  $\varepsilon_{\tau\tau}$ . The error bars represent  $1\sigma$  errors in any bin.  $\varepsilon_{e\tau} = 10^{-4}$ .

In the presence of NSI  $\bar{\nu}_e$  will arrive at the Earth as  $\bar{\nu}_1$  in cases *BI*, and as  $\bar{\nu}_2$  in case *AI* and *CIa*. Therefore its observation would exclude cases *B* and *CIb*. This distortion in the spectra could be measured by comparing the neutrino signal at two or more different detectors such that the neutrinos travel different distances through the Earth before reaching them [73, 74]. However these Earth matter effects can be also identified in a single detector [75, 76].

By analyzing the power spectrum of the detected neutrino events one can identify the presence of peaks located at the frequencies characterizing the modulation. These do not depend on the primary neutrino spectra, and can be determined to a good accuracy from the knowledge of the solar oscillation parameters, the Earth matter density, and the position of the SN in the sky [76]. The latter can be determined with sufficient precision even if the SN is optically obscured using the pointing capability of water Cherenkov neutrino detectors [81].

This method turns out to be powerful in detecting the modulations in the spectra due to Earth matter effects, and thus in ruling out cases *B* and *CIb*. However, the position of the peaks does not depend on how  $\bar{\nu}_e$  enters the Earth, as  $\bar{\nu}_1$  or  $\bar{\nu}_2$ . Hence it is not useful to discriminate



case  $AI$  and  $CIA$  from the cases  $A$ ,  $C$ , and  $BI$ .

The time dependence of  $Y_e$ , however, can transform case  $B$  into  $BI$ , and  $C$  with inverse hierarchy into  $CIB$ , leading respectively to an appearance and disappearance of these Earth matter effects. In case  $BI$  the presence of the shock wave modulation can spoil a clear identification of the Earth matter effects. Nevertheless, the disappearance of the Earth matter effects in the transition from case  $C$  to  $CIB$  allows us to pin down case  $CIB$ .

#### D. Neutronization burst

The prompt neutronization burst takes place during the first  $\sim 25$  ms after the core bounce with a typical full width half maximum of 5–7 ms and a peak luminosity of  $3.3\text{--}3.5 \times 10^{53}$  erg s $^{-1}$ . The striking similarity of the neutrino emission characteristics despite the variability in the properties of the pre-collapse cores is caused by a regulation mechanism between electron number fraction and target abundances for electron capture. This effectively establishes similar electron fractions in the inner core during collapse, leading to a convergence of the structure of the central part of the collapsing cores, with only small differences in the evolution of different progenitors until shock breakout [77, 78].

Taking into account that the SN will be likely to be obscured by dust and a good estimation of the distance will not be possible, the time structure of the detected neutrino signal should be used as signature for the neutronization burst. In Ref. [78] it was shown that such a time structure can be in principle cleanly seen in the case of a Megaton water Cherenkov detector. It was also shown how the time evolution of the signal depends strongly on the neutrino mixing scheme. In the absence of NSI the  $\nu_e$  peak could be observed provided that the  $\nu_e$  survival probability  $P_{\nu_e\nu_e}$  is not zero. As can be seen in Table I this happens for cases  $B$  and  $C$ . However for case  $A$  (normal mass hierarchy and “large”  $\vartheta_{13}$ ),  $\nu_e$  leaves the SN as  $\nu_3$ . This leads to a survival probability  $P_{\nu_e\nu_e} \approx \sin^2 \vartheta_{13} \lesssim 10^{-1}$ , and therefore the peak remains hidden.

Let us now consider the situation where NSI are present. For normal mass hierarchy  $\nu_e$ , which is born as  $\nu_2^m$  passes through three different resonances,  $I$ ,  $H$

and  $L$ . Whereas  $I$  and  $L$  will be adiabatic, the fate of  $H$  will depend on the value of  $\vartheta_{13}$ . For “large” values, case  $AI$ , the  $H$ -resonance will also be adiabatic. This implies that  $\nu_e$ ’s will leave as  $\nu_2$ , the survival probability will be  $P_{\nu_e\nu_e} \approx \sin^2 \vartheta_{12} \approx 0.3$ , and therefore the peak will be seen, as in cases  $B$  and  $C$ . If  $\vartheta_{13}$  happens to be very small, case  $CIA$ , then  $H$  will be strongly non-adiabatic and therefore  $\nu_e$  will leave the star as  $\nu_3$ . As a consequence the neutronization peak will not be seen.

For inverse mass hierarchy,  $\nu_e$  is born as  $\nu_1^m$  and traverses adiabatically  $I$  and  $L$ . This implies that they will leave the star as  $\nu_1$  and therefore the peak will also be observed. However now the survival probability will be larger,  $P_{\nu_e\nu_e} \approx \cos^2 \vartheta_{12} \approx 0.7$ . Thus for a given known normalization, i.e. the distance to the SN, one expects a larger number of events during the neutronization peak in this case. In Fig. 12 we show the expected number of events per time bin in a water Cherenkov detector in the case of a SN exploding at 10 kpc, for two different neutrino schemes,  $C$  and  $BI$ , and for different SN progenitor masses. One can see how the difference due to the larger survival probability is bigger than the typical error bars, associated to the lack of knowledge of the progenitor mass.

Two comments are in order. The neutronization  $\nu_e$  burst takes place during the first milliseconds, before strong deleptonization takes place. As a result, in contrast to other observables we have considered in this paper, here the  $I$ -resonance will only occur for  $\varepsilon^I \gtrsim 10^{-1}$ . On the other hand in the presence of additional NSI with electrons this would significantly affect the  $\nu - e$  cross sections, and consequently the results presented here.

## VI. SUMMARY

We have analyzed the possibility of observing clear signatures of non-standard neutrino interactions from the detection of neutrinos produced in a future galactic supernova.

In Secs. III and IV we have re-considered effect of  $\nu - d$  non-standard interactions on the neutrino propagation through the SN envelope within a three-neutrino framework. In contrast to previous works we have analyzed the neutrino evolution in both the more deleptonized in-

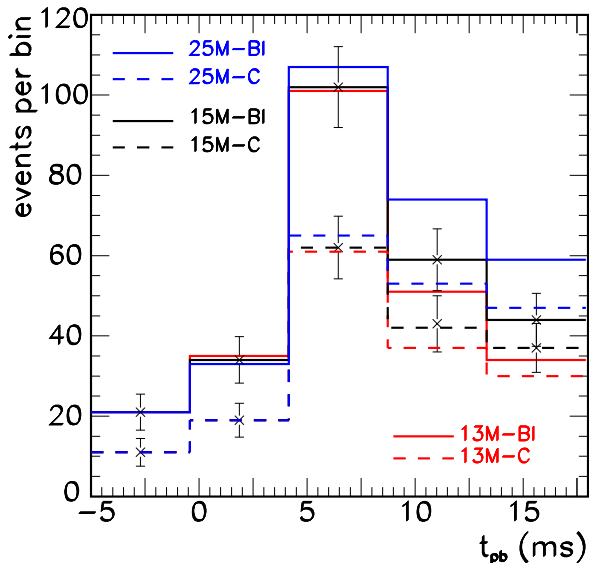


FIG. 12: Number of events from the elastic scattering on electrons, per time bin in a Megaton water Cherenkov detector for a SN at 10 kpc for cases *C* (dashed lines) and *BI* (solid lines). Different progenitor masses have been assumed:  $13 M_{\odot}$  (n13) in red,  $15 M_{\odot}$  (s15s7b2) in black, and  $25 M_{\odot}$  (s25a28) in blue. 1-sigma errors are also shown for the  $15 M_{\odot}$  case.

ner layers and the outer regions of the SN envelope. We have also taken into account the time dependence of the SN density and electron fraction profiles.

First we have found that the small values of the electron fraction typical of the former allows for internal NSI-induced resonant conversions, in addition to the standard MSW-H and MSW-L resonances of the outer envelope. These new flavor conversions take place for a relatively large range of NSI parameters, namely  $|\varepsilon_{\alpha\alpha}|$  between  $10^{-2} - 10^{-1}$ , and  $|\varepsilon_{e\tau}| \gtrsim \text{few} \times 10^{-5}$ , currently allowed by experiment. For this range of strengths, in particular  $\varepsilon_{\tau\tau}$ , non-standard interactions can significantly affect the adiabaticity of the *H*-resonance. On the other hand the NSI-induced resonant conversions may also lead to the modulation of the  $\bar{\nu}_e$  spectra as a result of the time dependence of the electron fraction.

In Sec. V we have studied the possibility of detecting NSI effects in a Megaton water Cherenkov detector using the modulation effects in the  $\bar{\nu}_e$  spectrum due to (i) the passage of shock waves through the SN envelope, (ii) the time dependence of the electron fraction and (iii) the

Earth matter effects; and, finally, through the possible detectability of the neutronization  $\nu_e$  burst. Note that observable (ii) turns out to be complementary to the observation of the shock wave passage, (i), and offers the possibility to probe NSI effects also for normal hierarchy neutrino spectra.

In Table II we summarize the results obtained for different neutrino schemes. We have found that observable (i) can clearly indicate the existence of NSI in the case of inverse mass hierarchy and large  $\vartheta_{13}$  (case *BI*). On the other hand, observable (ii) allows for an identification of NSI effects in the other cases, normal mass hierarchy (cases *AI* and *CIa*) and inverse mass hierarchy and small  $\vartheta_{13}$  (case *CIb*). Therefore a positive signal of either observable (i) or (ii) would establish the existence of NSI. In the latter case this would, however, leave a degeneracy among cases *AI*, *CIa*, and *CIb*. Such degeneracy can be broken with the help of observables (iii) and the observation of the neutronization  $\nu_e$  burst. The detection of Earth matter effects during the whole supernova neutrino signal would rule out case *CIb* since, as discussed in Sec. VC, a disappearance of Earth matter effects would take place due to a transition from *C* to *CIb*. Finally, the (non) observation of the neutronization burst can be used to distinguish between cases *AI* and *CIa*.

Similarly, other degeneracies in Table II may be lifted by suitably combining different observables. For example, a negative of observable (ii) could mean either negligible NSI strengths or (NU) NSI parameter values so large that the internal resonance is always present. In this case one could use the observation of the neutronization burst in order to establish the presence of NSI for the case of inverse mass hierarchy. In addition the observation of the shock wave imprint in the  $\bar{\nu}_e$  spectrum would provide additional information on  $\vartheta_{13}$ .

In conclusion, by suitably combining all observables one may establish not only the presence of NSI, but also the mass hierarchy and probe the magnitude of  $\vartheta_{13}$ .

### Acknowledgments

The authors wish to thank H-Th. Janka, O. Miranda, S. Pastor, Th. Schwetz, and M. Tórtola for fruitful discussions. Work supported by the Spanish grant FPA2005-

Scheme	Hierarchy	$\sin^2 \vartheta_{13}$	NSI	shock	$Y_e$	Earth	$\nu_e$ burst
<i>A</i>	normal	$\gtrsim 10^{-4}$	No	No	No	Yes	No
<i>B</i>	inverted	$\gtrsim 10^{-4}$	No	Yes	No	No	Yes
<i>C</i>	any	$\lesssim 10^{-6}$	No	No	No	Yes	Yes
<i>AI</i>	normal	$\gtrsim 10^{-4}$	Yes	No	Yes	Yes	Yes
<i>BI</i>	inverted	$\gtrsim 10^{-4}$	Yes	Yes*	No	Yes	Yes*
<i>CIa</i>	normal	$\lesssim 10^{-6}$	Yes	No	Yes	Yes	No
<i>CIb</i>	inverted	$\lesssim 10^{-6}$	Yes	No	Yes	No	Yes*

TABLE II: Expectations for the observables discussed in the text: modulation of the  $\bar{\nu}_e$  spectrum due to the shock wave passage, the time variation of  $Y_e$ , the Earth effect, and the observation of the  $\nu_e$  burst within various neutrino schemes. Asterisks indicate that the effect differs from that expected in the absence of NSI. See text.

01269 and European Network of Theoretical Astroparticle Physics ILIAS/N6 under contract number RII3-CT-2004-506222. A. E. has been supported by a FPU grant from the Spanish Government. R. T. has been supported by the Juan de la Cierva program from the Spanish Government and by an ERG from the European Commission.

## References

- 
- [1] KamLAND collaboration, K. Eguchi *et al.*, Phys. Rev. Lett. **90**, 021802 (2003), [hep-ex/0212021].
- [2] S. Pakvasa and J. W. F. Valle, hep-ph/0301061, Proc. of the Indian National Academy of Sciences on Neutrinos, Vol. 70A, No.1, p.189 - 222 (2004), Eds. D. Indumathi, M.V.N. Murthy and G. Rajasekaran.
- [3] V. Barger, D. Marfatia and K. Whisnant, hep-ph/0308123.
- [4] KamLAND collaboration, T. Araki *et al.*, Phys. Rev. Lett. **94**, 081801 (2004).
- [5] M. Maltoni, T. Schwetz, M. A. Tortola and J. W. F. Valle, New J. Phys. **6**, 122 (2004), Appendix C in hep-ph/0405172 (v5) provides updated neutrino oscillation results taking into account new SSM, new SNO salt data, latest K2K and MINOS data; previous works by other groups are referenced therein.
- [6] J. Schechter and J. W. F. Valle, Phys. Rev. **D22**, 2227 (1980).
- [7] J. W. F. Valle, J. Phys. Conf. Ser. **53**, 473 (2006), [hep-ph/0608101], Review based on lectures at the Corfu Summer Institute on Elementary Particle Physics in September 2005.
- [8] J. Schechter and J. W. F. Valle, Phys. Rev. **D24**, 1883 (1981), Err. D25, 283 (1982).
- [9] C.-S. Lim and W. J. Marciano, Phys. Rev. **D37**, 1368 (1988).
- [10] E. K. Akhmedov, Phys. Lett. **B213**, 64 (1988).
- [11] L. Wolfenstein, Phys. Rev. **D17**, 2369 (1978).
- [12] Mikheev, S. P. and Smirnov, A. Yu., (Editions Frontières, Gif-sur-Yvette, 1986, p.355.), 86 Massive Neutrinos in Astrophysics and Particle Physics, Proceedings of the Sixth Moriond Workshop, ed. by Fackler, O. and Tran Thanh Van, J.
- [13] J. W. F. Valle, Phys. Lett. **B199**, 432 (1987).
- [14] R. N. Mohapatra and J. W. F. Valle, Phys. Rev. **D34**, 1642 (1986).
- [15] J. Bernabeu *et al.*, Phys. Lett. **B187**, 303 (1987).
- [16] G. C. Branco, M. N. Rebelo and J. W. F. Valle, Phys. Lett. **B225**, 385 (1989).
- [17] N. Rius and J. W. F. Valle, Phys. Lett. **B246**, 249 (1990).
- [18] F. Deppisch and J. W. F. Valle, Phys. Rev. **D72**, 036001 (2005), [hep-ph/0406040].
- [19] A. Zee, Phys. Lett. **B93**, 389 (1980).
- [20] K. S. Babu, Phys. Lett. **B203**, 132 (1988).
- [21] L. J. Hall, V. A. Kostelecky and S. Raby, Nucl. Phys. **B267**, 415 (1986).
- [22] M. Malinsky, J. C. Romao and J. W. F. Valle, Phys. Rev. Lett. **95**, 161801 (2005), [hep-ph/0506296].
- [23] A. B. McDonald, astro-ph/0406253.
- [24] K. Scholberg, astro-ph/0701081.
- [25] LSND, L. B. Auerbach *et al.*, Phys. Rev. **D63**, 112001 (2001), [hep-ex/0101039].
- [26] MUNU, Z. Daraktchieva *et al.*, Phys. Lett. **B564**, 190 (2003), [hep-ex/0304011].
- [27] CHARM, J. Dorenbosch *et al.*, Phys. Lett. **B180**, 303 (1986).
- [28] CHARM-II, P. Vilain *et al.*, Phys. Lett. **B335**, 246 (1994).
- [29] NuTeV, G. P. Zeller *et al.*, Phys. Rev. Lett. **88**, 091802 (2002), [hep-ex/0110059].
- [30] V. D. Barger, R. J. N. Phillips and K. Whisnant, Phys. Rev. **D44**, 1629 (1991).
- [31] S. Davidson, C. Pena-Garay, N. Rius and A. Santamaria, JHEP **03**, 011 (2003), [hep-ph/0302093].

- [32] J. Barranco, O. G. Miranda, C. A. Moura and J. W. F. Valle, *Phys. Rev.* **D73**, 113001 (2006), [hep-ph/0512195].
- [33] Z. Berezhiani and A. Rossi, *Phys. Lett.* **B535**, 207 (2002), [hep-ph/0111137].
- [34] A. Friedland, C. Lunardini and C. Pena-Garay, *Phys. Lett.* **B594**, 347 (2004), [hep-ph/0402266].
- [35] M. M. Guzzo, P. C. de Holanda and O. L. G. Peres, *Phys. Lett.* **B591**, 1 (2004), [hep-ph/0403134].
- [36] O. G. Miranda, M. A. Tortola and J. W. F. Valle, *JHEP* **10**, 008 (2006), [hep-ph/0406280].
- [37] N. Fornengo *et al.*, *Phys. Rev.* **D65**, 013010 (2002), [hep-ph/0108043].
- [38] A. Friedland, C. Lunardini and M. Maltoni, *Phys. Rev.* **D70**, 111301 (2004), [hep-ph/0408264].
- [39] A. Friedland and C. Lunardini, *Phys. Rev.* **D72**, 053009 (2005), [hep-ph/0506143].
- [40] G. Mangano *et al.*, *Nucl. Phys.* **B756**, 100 (2006), [hep-ph/0607267].
- [41] S. K. Katsanevas, talk at Workshop on Neutrino Oscillation Physics (NOW 2006), Otranto, Lecce, Italy, 9-16 Sep 2006.
- [42] P. S. Amanik, G. M. Fuller and B. Grinstein, *Astropart. Phys.* **24**, 160 (2005), [hep-ph/0407130].
- [43] P. S. Amanik and G. M. Fuller, astro-ph/0606607.
- [44] S. P. Mikheev and A. Y. Smirnov, *Sov. J. Nucl. Phys.* **42**, 913 (1985).
- [45] S. P. Mikheev and A. Y. Smirnov, *Nuovo Cim.* **C9**, 17 (1986).
- [46] H. Nunokawa, Y. Z. Qian, A. Rossi and J. W. F. Valle, *Phys. Rev.* **D54**, 4356 (1996), [hep-ph/9605301].
- [47] H. Nunokawa, A. Rossi and J. W. F. Valle, *Nucl. Phys.* **B482**, 481 (1996), [hep-ph/9606445].
- [48] S. Mansour and T.-K. Kuo, *Phys. Rev.* **D58**, 013012 (1998), [hep-ph/9711424].
- [49] S. Bergmann and A. Kagan, *Nucl. Phys.* **B538**, 368 (1999), [hep-ph/9803305].
- [50] G. L. Fogli, E. Lisi, A. Mirizzi and D. Montanino, *Phys. Rev.* **D66**, 013009 (2002), [hep-ph/0202269].
- [51] T.-K. Kuo and J. T. Pantaleone, *Phys. Rev.* **D37**, 298 (1988).
- [52] S. Bergmann, *Nucl. Phys.* **B515**, 363 (1998), [hep-ph/9707398].
- [53] P. Huber, T. Schwetz and J. W. F. Valle, *Phys. Rev. Lett.* **88**, 101804 (2002), [hep-ph/0111224].
- [54] P. Huber, T. Schwetz and J. W. F. Valle, *Phys. Rev.* **D66**, 013006 (2002), [hep-ph/0202048].
- [55] Particle Data Group, W. M. Yao *et al.*, *J. Phys.* **G33**, 1 (2006).
- [56] F. J. Botella, C. S. Lim and W. J. Marciano, *Phys. Rev.* **D35**, 896 (1987).
- [57] S. E. Woosley, A. Heger and T. A. Weaver, *Reviews of Modern Physics* **74**, 1015 (2002).
- [58] R. C. Schirato, G. M. Fuller, . U. . LANL), UCSD and LANL), astro-ph/0205390.
- [59] G. L. Fogli, E. Lisi, D. Montanino and A. Mirizzi, *Phys. Rev.* **D68**, 033005 (2003), [hep-ph/0304056].
- [60] R. Tomas *et al.*, *JCAP* **0409**, 015 (2004), [astro-ph/0407132].
- [61] C. Y. Cardall, astro-ph/0701831.
- [62] H. A. Bethe, J. H. Applegate and G. E. Brown, *Astrophys. J.* **241**, 343 (1980).
- [63] A. Burrows and T. J. Mazurek. *Astrophys. J.* **259**, 330 (1982).
- [64] H. Th. Janka, private communication.
- [65] T.-K. Kuo and J. T. Pantaleone, *Rev. Mod. Phys.* **61**, 937 (1989).
- [66] M. Kachelriess and R. Tomas, hep-ph/0412100.
- [67] M. Liebendoerfer *et al.*, *Phys. Rev.* **D63**, 103004 (2001), [astro-ph/0006418].
- [68] M. Rampp and H. T. Janka, *Astron. Astrophys.* **396**, 361 (2002), [astro-ph/0203101].
- [69] T. A. Thompson, A. Burrows and P. A. Pinto, *Astrophys. J.* **592**, 434 (2003), [astro-ph/0211194].
- [70] K. Sumiyoshi *et al.*, *Astrophys. J.* **629**, 922 (2005), [astro-ph/0506620].
- [71] Y.-Z. Qian, *Prog. Part. Nucl. Phys.* **50**, 153 (2003), [astro-ph/0301422].
- [72] J. Pruet, S. E. Woosley, R. Buras, H.-T. Janka and R. D. Hoffman, *Astrophys. J.* **623**, 325 (2005), [astro-ph/0409446].
- [73] C. Lunardini and A. Y. Smirnov, *Nucl. Phys.* **B616**, 307 (2001), [hep-ph/0106149].
- [74] A. S. Dighe, M. T. Keil and G. G. Raffelt, *JCAP* **0306**, 005 (2003), [hep-ph/0303210].
- [75] A. S. Dighe, M. T. Keil and G. G. Raffelt, *JCAP* **0306**, 006 (2003), [hep-ph/0304150].
- [76] A. S. Dighe, M. Kachelriess, G. G. Raffelt and R. Tomas, *JCAP* **0401**, 004 (2004), [hep-ph/0311172].
- [77] K. Takahashi, K. Sato, A. Burrows and T. A. Thompson, *Phys. Rev.* **D68**, 113009 (2003), [hep-ph/0306056].
- [78] M. Kachelriess *et al.*, *Phys. Rev.* **D71**, 063003 (2005), [astro-ph/0412082].
- [79] M. T. Keil, PhD thesis TU München 2003 [astro-ph/0308228].
- [80] M. T. Keil, G. G. Raffelt and H. T. Janka, *Astrophys. J.* **590** (2003) 971 [astro-ph/0208035].
- [81] R. Tomas, D. Semikoz, G. G. Raffelt, M. Kachelriess and A. S. Dighe, *Phys. Rev.* **D68**, 093013 (2003), [hep-ph/0307050].
- [82] H. Nunokawa, V. B. Semikoz, A. Y. Smirnov and J. W. F. Valle, *Nucl. Phys.* **B501**, 17 (1997), [hep-ph/9701420].
- [83] H. Duan, G. M. Fuller, J. Carlson and Y.-Z. Qian, *Phys. Rev.* **D74**, 105014 (2006), [astro-ph/0606616].
- [84] H. Duan, G. M. Fuller, J. Carlson and Y.-Z. Qian, *Phys. Rev. Lett.* **97**, 241101 (2006), [astro-ph/0608050].
- [85] S. Hannestad, G. G. Raffelt, G. Sigl and Y. Y. Y. Wong,

- Phys. Rev. **D74**, 105010 (2006), [astro-ph/0608695].
- [86] G. G. Raffelt and G. G. R. Sigl, hep-ph/0701182.
- [87] A. B. Balantekin, J. M. Fetter and F. N. Loreti, Phys. Rev. **D54**, 3941 (1996), [astro-ph/9604061].
- [88] H. Nunokawa, A. Rossi, V. B. Semikoz and J. W. F. Valle, Nucl. Phys. **B472**, 495 (1996), [hep-ph/9602307].
- [89] G. L. Fogli, E. Lisi, A. Mirizzi and D. Montanino, JCAP **0606**, 012 (2006), [hep-ph/0603033].
- [90] A. Friedland and A. Gruzinov, astro-ph/0607244.
- [91] Axial couplings would affect neutrino propagation in polarized media, see Ref. [82].
- [92] However we have confined ourselves to values of  $\varepsilon_{e\alpha}$  small enough not to lead to drastic consequences during the core collapse.
- [93] For the sake of simplicity we will omit the superindex  $V$ .
- [94] The importance of collective flavor neutrino conversions driven by neutrino-neutrino interactions has been recently noted in Refs. [83, 84, 85, 86]. Here we consider only the case where the effective potential felt by neutrinos comes from their interactions with electrons, protons and neutrons. In a future work we plan to include this effect and have a complete picture of the neutrino propagation.
- [95] Here we neglect the possible effects of density fluctuations [87, 88] taking place during the shock wave propagation. For a detailed study of the phenomenological consequences see Refs. [89, 90].
- [96] The alternative condition  $H'_{ee} = H'_{\mu\mu}$  would give rise to another internal resonance which can be studied using the same method. For brevity, we will not pursue this in this paper.
- [97] Note that, in the limit of high densities one recovers the rotation angle obtained for the internal  $I$ -resonance  $\vartheta''_{23} \rightarrow \vartheta'_{23}$  after neglecting the kinetic terms.
- [98] For the case of NSI with electrons both the vector and axial components of  $\varepsilon_{\alpha\beta}^e$  will contribute to the  $\nu - e$  cross section.
- [99] We assume that for the values of the NSI parameters considered the initial neutrino spectra do not significantly change.